TABLE 1. Demographic information and risk category of persons infected with the CRF08_BC and CRF07_BC viruses

Virus strain and location	No. of sequences	No. of patients at risk for:[a]	
		IDU	Sexual behavior
CRF08_BC			
Yunnan	31	26	5
Guangxi	44	44	
Liaoning	5	2	3
Gansu	1	UNK	UNK
CRF07_BC			
Yunnan	10	7	3
Xinjiang	6	5	1
Liaoning[b]	6	4	2

[a] UNK, unknown.
[b] Five patients recruited in Liaoning are reported as having acquired HIV infection outside Liaoning: four in Guangdong and one in Sichuan.

In this study, we investigated the spatial and temporal spread of HIV-1 CRF08_BC and CRF07_BC in China by reconstructing the evolutionary histories of these strains using recently developed Bayesian analysis methods. In addition, we also assessed the phylodynamics of the subtype C lineage of Indian origin in order to provide a more comprehensive picture of the movement of subtype C and its related recombinants in the region. Here, we demonstrate and provide a timescale for the eastwards spread of HIV/AIDS in East Asia, and we highlight the significance of HIV-1 evolutionary history upon viral epidemiology, migration and molecular taxonomy.

MATERIALS AND METHODS

HIV-1 CRF08_BC and CRF07_BC sequence information. HIV-1 CRF08_BC nucleotide sequences with known sampling dates were retrieved from the Los Alamos HIV Sequence Database (www.hiv.lanl.gov). Eighty-one CRF08_BC sequences, including the reference strains previously reported by our laboratory and others, were isolated from the provinces of Yunnan (n = 31; southwestern China), Guangxi (n = 44; southern China), Gansu (n = 1; northwestern China), and Liaoning (n = 5; northeastern China) (11, 15, 17, 26, 32, 48, 49). Samples from Yunnan province were collected mainly from Kunming, Honghe, and Wenshan prefectures, while isolates from Baise city, Binyang, and Pingxiang counties represented the Guangxi autonomous region. Liaoning sequences were derived from the provincial capital Shenyang. The nonrecombinant *gag-pol* region of CRF08_BC was selected for codon-based alignment, phylogenetic reconstruction, and coalescent analysis (14). This spans the region from p2 in *gag* to the reverse transcriptase in *pol* (strain HXB2 nucleotides 1918 to 2852; 921 bp in length) and is of subtype C origin. Similarly, 22 CRF07_BC sequences with known sampling years were retrieved from the database. These CRF07_BC sequences were isolated from Yunnan (n = 10), Xinjiang (n = 6; northwestern China), and Liaoning (n = 6) provinces (11, 17, 22, 32, 38, 48, 49). Except for five sequences from Xinjiang, all of the CRF07_BC nucleotide sequences have been previously reported by our laboratory. Although the Liaoning patients were recruited in the provincial capital Shenyang, interviews with the patients revealed that only one was possibly infected in Liaoning, whereas four patients reported having acquired the infection in Guangdong (southeastern) province and one patient in Sichuan (central) province. The 420-bp nonrecombinant *gag* region of CRF07_BC, which is of subtype C origin and encompasses the p17 and partial p24 proteins (HXB2 nucleotides 790 to 1218) was aligned for phylogenetic and evolutionary analyses. Demographic information and risk category for the persons from whom studied isolates were obtained are summarized in Table 1.

Bayesian MCMC evolutionary analyses. Genome region-specific rates of evolution were obtained from a reference set of subtype C sequences using BEAST, version 1.4 (7), a program that employs a Markov chain Monte Carlo (MCMC) algorithm to estimate evolutionary parameters. To perform these analyses, subtype C regions of *gag-pol* and *gag* that correspond to the nonrecombinant subtype C segments of CRF08_BC and CRF07_BC, respectively, were retrieved from the HIV sequence database. The resulting heterochronous reference data set contains 41 subtype C sequences sampled between 1989 and 2005, a date range of about 17 years. Maximum-likelihood phylogenies were estimated for each subgenomic region of CRF08_BC and CRF07_BC and for the heterochronous subtype C reference data set using PAUP*, version 4.0 beta (40), and BEAST, version 1.4 (7). All nucleotide alignments are available from the authors upon request.

Strict and relaxed molecular clock (5) analyses were performed under the Hasegawa-Kishino-Yano (HKY) (12) and general time-reversible (33) substitution models, with a gamma-distributed model of among-site rate variation with four rate categories (Γ_4) (50). Here, the demographic model component of the BEAST analysis was not of interest, and, hence, it was treated as a nuisance parameter. Each analysis was therefore repeated using constant size, exponential, and logistic growth models in order to investigate the degree to which dating estimates are affected by the demographic model chosen (6). Each MCMC analysis was run for 20 million steps and sampled every 10,000 states. The posterior densities were calculated with 10% burn-in and checked for convergence using Tracer, version 1.4 (28). The posterior distribution of evolutionary rate obtained from the heterochronous reference data set was subsequently incorporated as a prior distribution for the evolutionary rate in the HIV-1 CRF08_BC and CRF07_BC analyses, thereby placing a timescale on the histories of these strains and enabling an estimation of the time to the most recent common ancestor (tMRCA) for the strains (27).

In order to test the possible effects of intrasubtype recombination on the estimated dates, we applied in BEAST a multiple unlinked locus model that allows independent coalescent pathways for different gene loci (16). The "linked" *gag-pol* gene was partitioned into two unlinked loci of equivalent length, denoted locus 1 (HXB2 nucleotides 1918 to 2390) and 2 (HXB2 nucleotides 2391 to 2852), and their tMRCAs were estimated in the Bayesian coalescent framework assuming a shared demographic history among all loci. Genealogical correlation between the linked and unlinked loci was evaluated by assessing their divergence dates.

Evolutionary analysis of subtype C. HIV-1 subtype C, probably of Indian origin, was identified as a major circulating strain in China in the early 1990s and is believed to be the putative parent for CRF08_BC and CRF07_BC (19, 20). To assess the divergence times of subtype C in both India and China, "pure" nonrecombinant subtype C genetic regions from 12 nearly full-length subtype C sequences of Indian origin (including a nearly full-length sequence from Myanmar [41]) were retrieved from the HIV Sequence Database. Additionally, 112 subtype C-related *env* sequences (HXB2 nucleotides 6984 to 7328; 336 bp) isolated from China were retrieved; these Chinese sequences were typed as subtype C (n = 14), CRF08_BC (n = 87), and CRF07_BC (n = 10) and one B'/C unique recombinant form. The methods described above were used to estimate phylogenies, genome region-specific evolutionary rates, and tMRCAs of the Indian and Chinese strains from the *gag-pol* and/or *env* genes. Furthermore, select subtype C sequences from other localities (31 full-length sequences from Africa and also Brazil) were also studied in order to assess the time of origin of the global HIV-1 subtype C.

RESULTS

A total of 103 HIV-1 B'/C circulating recombinant forms were retrieved from at least five provinces/autonomous regions representing a relatively wide range of locations across mainland China, three of which have the highest recorded HIV prevalences in the country (Yunnan, Guangxi, and Xinjiang) (23). Nucleotide sequences of the nonrecombinant regions of HIV-1 CRF08_BC (n = 81) and CRF07_BC (n = 22) from IDU (86.3%) and sexual risk patients (13.7%) were selected, codon aligned, and analyzed using likelihood and Bayesian approaches to determine their evolutionary relationships in various regions. Additionally, subtype C or subtype C-related sequences from India and China (n = 124) were also analyzed to determine the time of origin of these lineages.

Phylogenetic reconstruction of the *gag-pol* gene (Fig. 1a) showed that all CRF08_BC sequences grouped in a single clade containing isolates from four Chinese regions: Yunnan, Gansu, Liaoning, and Guangxi (Baise city and Binyang and

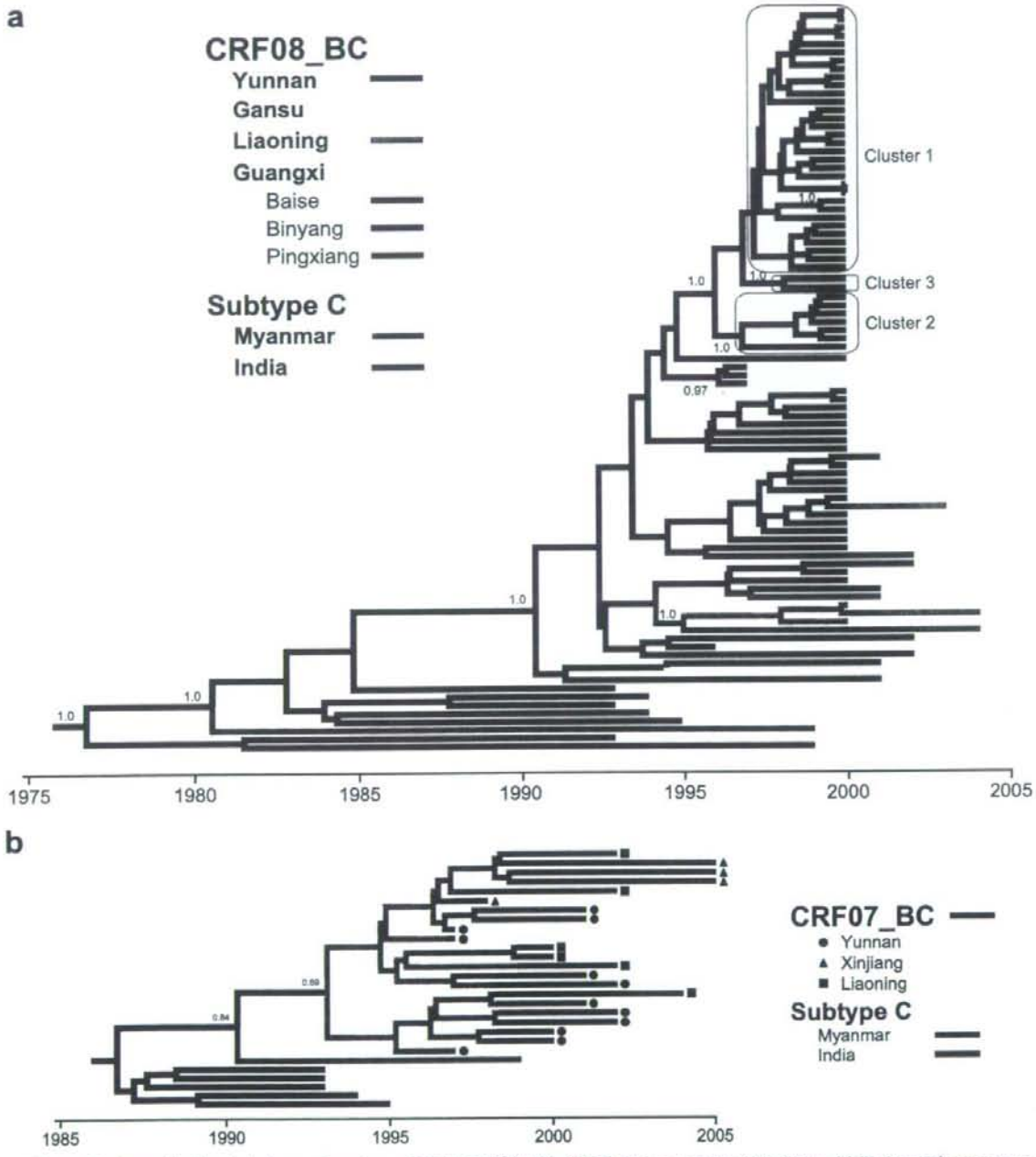

FIG. 1. Maximum-likelihood phylogenetic analyses of HIV-1 CRF08_BC, CRF07_BC, and subtype C in China. (a) Phylogenetic reconstructions of CRF08_BC *gag-pol* genes (HXB2 nucleotides 1918 to 2852) isolated from HIV-1 patients in the Yunnan (Kunming, Honghe, and Wenshan), Gansu, Liaoning (Shenyang), and Guangxi (Baise, Binyang, and Pingxiang) regions of China. (b) Maximum clade credibility trees of the HIV-1 CRF07_BC sequences from Yunnan, Xinjiang, and Liaoning provinces, based on the *gag* gene (HXB2 nucleotides 790 to 1218). (c) The *env* (HXB2 nucleotides 6984 to 7328) phylogeny of subtype C, CRF08_BC, CRF07_BC, and a B'/C unique recombinant form isolated from China. Ancestral relationships are estimated using PAUP*, version 4.0 beta (40), and BEAST, version 1.4 (7). Subtype C of Indian origin, thought to be the putative parent of both CRF08_BC and CRF07_BC (19, 20), is also included. The CRF08_BC *gag-pol* and CRF07_BC *gag* tree branches are colored according to their respective geographical locations while the *env* tree branches show the respective HIV-1 subtype/CRF. Posterior probabilities greater than 0.5 are shown at their respective nodes.

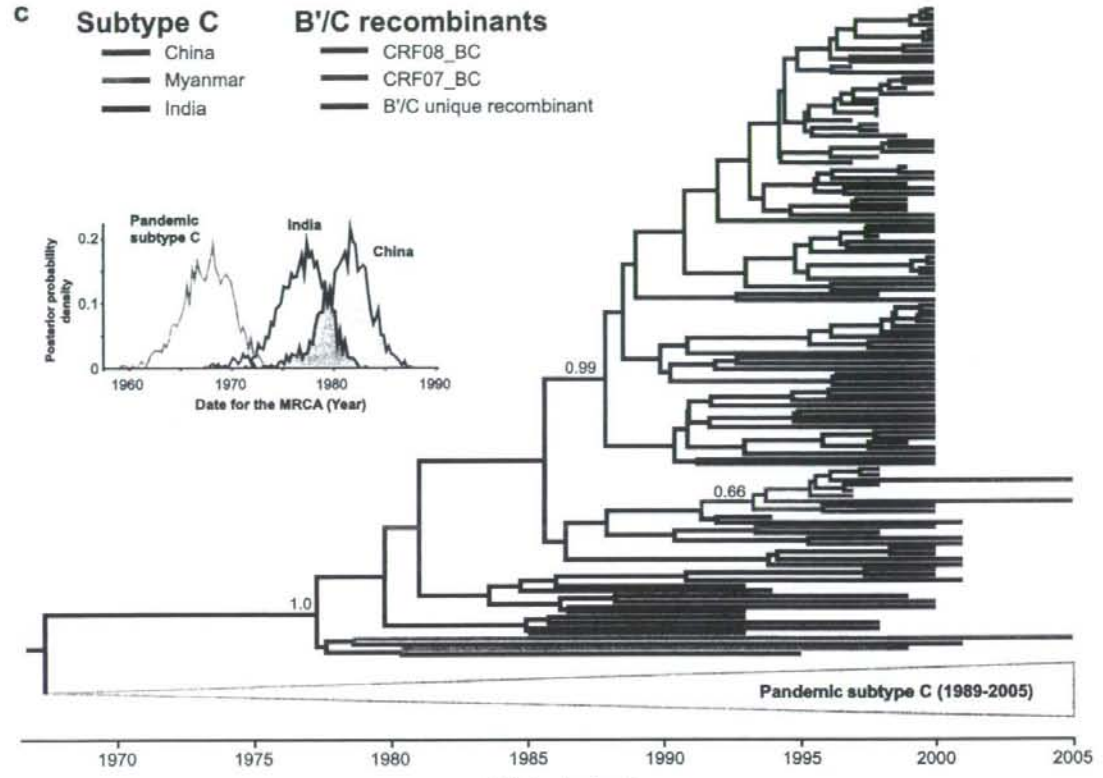

FIG. 1—*Continued.*

Pingxiang counties). These sequences were descended from subtype C isolates of Indian origin, confirming the parental relationship of Indian subtype C with respect to CRF08_BC. Yunnan sequences collected from different prefectures (Kunming, Honghe, and Wenshan) (49) were largely intermingled with sequences from Gansu, Liaoning, and Guangxi (Baise), suggesting close relationships among these sequences. However, other sequences from Binyang county (and also Pingxiang) in Guangxi formed a distinct monophyletic cluster that diverged from the Yunnan/Baise isolates and further bifurcated into three major clusters (indicated as clusters 1 to 3). Cluster 1 contained sequences from Binyang (n = 30) and Pingxiang (n = 2), while clusters 2 and 3 contained seven and two Binyang sequences, respectively. The robustness of each cluster was supported by high posterior clade probabilities ($P > 0.95$). Similarly, CRF08_BC sequences from Liaoning province (except that of one subject who acquired the infection in Yunnan) also formed a single cluster.

Bayesian analyses under different evolutionary models estimated consistent mean rates of evolution (μ) for the CRF08_BC *gag-pol* gene, in the range of 1.7×10^{-3} to 1.8×10^{-3} substitutions/site/year. This range of rates was included as a prior probability distribution in subsequent analyses in order to calculate the tMRCA of the respective CRF08_BC clusters. When the constant size population model and HKY substitution model were used, the Yunnan (and Gansu) clusters were dated to 1990.3 (95% credible region [CR], 1988.6 to 1991.9) (Table 2). CRF08_BC was probably introduced later into Baise city in neighboring Guangxi around 1995.5 (95% CR, 1994.3 to 1996.5). This is in agreement with previous epidemiological investigations, which reported the first outbreaks of CRF08_BC (then classified as subtype C based on *env* gene sequencing) in this area (26, 51). Interestingly, the tMRCA of the Liaoning cluster is estimated at 1995.6 (95% CR, 1993.4 to 1997.5), comparable to that of Guangxi, and sequences from both these regions trace their origins to Yunnan. This suggests that the epidemics in Liaoning, an area with low HIV/AIDS prevalence, and Guangxi could have started at almost the same time. As shown in the *gag-pol* phylogeny (Fig. 1a), subsequent spread of CRF08_BC among the IDU populations in Binyang and Pingxiang involved at least three viral lineages (clusters 1 to 3) descended from the Yunnan or Baise sequences between 1997 and 1999 (Table 2). In addition, all Binyang and Pingxiang sequences contained signature amino acid deletions in *gag* (p7, p1, and p6) and in reverse transcriptase at position P25 (amino acid alignment not shown) that were not found in other CRF08_BC sequences, suggesting a shared common ancestor for these strains. Overall, the evolutionary and statistical as-

TABLE 2. Evolutionary characteristics of CRF08_BC, CRF07_BC, and subtype C

HIV-1 strain or subtype and location	Genetic region	Value (HPD) of the evolutionary parameter according to the indicated model[a]					
		HKY+Γ_4 constant size		HKY+Γ_4 exponential growth		HKY+Γ_4 logistic growth	
		Rate of evolution	tMRCA	Rate of evolution	tMRCA	Rate of evolution	tMRCA
CRF08_BC							
Yunnan and Gansu	*gag-pol*	1.8 (1.4, 2.3)	1990.3 (1988.6, 1991.9)	1.8 (1.4, 2.3)	1989.8 (1988.0, 1991.6)	1.7 (1.3, 2.1)	1989.3 (1987.3, 1991.0)
Liaoning			1995.6 (1993.4, 1997.5)		1995.2 (1993.0, 1997.4)		1995.1 (1992.6, 1997.3)
Guangxi							
Baise			1995.5 (1994.3, 1996.5)		1995.3 (1994.1, 1996.6)		1995.3 (1993.8, 1996.4)
Binyang							
Cluster 1			1997.1 (1996.3, 1997.9)		1996.9 (1996.0, 1997.7)		1996.8 (1995.9, 1997.6)
Cluster 2			1998.3 (1997.0, 1999.4)		1998.0 (1996.6, 1999.3)		1998.0 (1996.6, 1999.3)
Cluster 3			1998.5 (1997.3, 1999.5)		1998.4 (1997.1, 1999.5)		1998.3 (1997.1, 1999.4)
Pingxiang			1999.3 (1998.5, 1999.9)		1999.2 (1998.3, 1999.9)		1999.2 (1998.3, 1999.9)
CRF07_BC							
Yunnan, Xinjiang, and Liaoning[b]	*gag*	4.4 (3.1, 5.7)	1993.3 (1991.2, 1995.2)	3.5 (2.1, 4.7)	1989.4 (1986.2, 1992.2)	3.9 (2.6, 5.1)	1992.0 (1989.5, 1994.3)
Taiwan[c]							
Tainan (Southern)	*env*	4.8 (3.0, 6.6)	1999.7 (1998.2, 2001.1)	4.9 (3.0, 6.6)	1999.7 (1998.2, 2001.0)	4.2 (2.6, 5.9)	1999.1 (1997.5, 2000.6)
Taipei and Nantou (northern-central)			2002.1 (2001.3, 2002.9)		2002.1 (2001.1, 2002.8)		2001.7 (2000.7, 2002.7)
Subtype C							
Global	*gag-pol*	1.8 (1.4, 2.3)	1967.6 (1962.5, 1972.0)	1.8 (1.4, 2.3)	1966.9 (1962.1, 1971.6)	1.7 (1.3, 2.1)	1970.3 (1967.0, 1973.7)
India	*gag-pol*	1.8 (1.4, 2.3)	1979.7 (1976.9, 1982.3)	1.8 (1.4, 2.3)	1979.5 (1976.3, 1982.6)	1.7 (1.3, 2.1)	1977.8 (1974.7, 1980.7)
	env	5.6 (3.1, 7.6)	1976.9 (1972.1, 1981.5)	5.2 (3.1, 7.0)	1978.7 (1974.8, 1982.8)	5.2 (3.3, 7.3)	1978.2 (1973.9, 1982.1)
China	*env*	5.6 (3.1, 7.6)	1981.2 (1976.7, 1985.9)	5.2 (3.1, 7.0)	1982.3 (1978.8, 1985.5)	5.2 (3.3, 7.3)	1982.0 (1978.1, 1985.2)

[a] Rates of evolution are expressed as 10^{-3} nucleotide substitutions per site per year. The 95% highest posterior density (HPD) confidence intervals are given in parentheses.
[b] Five patients recruited in Liaoning are reported as having acquired HIV infection outside Liaoning (see Table 1).
[c] Constant size and exponential growth analyses based on the hypervariable region-stripped *env* gene previously described (43).

sumptions applied in the coalescence analyses have almost no effect on the estimated dates (results generated under the general time-reversible nucleotide substitution model are shown in Table S1 in the supplemental material). In addition to strict molecular clock analyses, we also explored the relaxed phylogenetic method (5) to estimate the divergence times for each data set. The results, under selected evolutionary priors, were comparable to those described above (see Fig. S1 in the supplemental material for a summary). Our analysis reconstructs the chronological events of HIV-1 expansion by retracing the north-eastward and eastward migration of CRF08_BC to Liaoning and Guangxi, respectively, most likely from a common source in Yunnan province. However, we note that the estimated coalescence times, particularly for clusters with a small number of sequences, may be biased and hence more recent than the date of outbreak. This is because, among other factors, the extant virus diversity has been partially sampled; alternatively, the founding/parental lineages of the outbreak have since become extinct or are yet to be discovered (1, 43).

Conversely, all *gag* sequences of CRF07_BC from Yunnan, Xinjiang, and Liaoning formed a single cluster, with subtype C isolates of Indian origin paraphyletic with respect to CRF07_BC (Fig. 1b). Coalescence analyses under a constant size population model (estimated evolutionary rate, $\mu = 4.4 \times 10^{-3}$ substitutions/site/year) imply that the common ancestor of the Chinese CRF07_BC isolates existed around 1993.3 (95% CR, 1991.2 to 1995.2) (Table 2). This is in agreement with previous studies, based on the *env* gene, which dated the divergence time of CRF07_BC to about 1993 (43). The exponential and logistic demographic model gave slightly lower substitution rates and hence older MRCA estimates. Harmonic means of the coalescent likelihood estimated using marginal likelihood analysis (39), however, showed that other tree models do not significantly fit the *gag* data set better than the constant size population model ($\log_{10}$ Bayes factors of <3.0), suggesting that there could be insufficient information in the data to fit a more complex model. The logistic model meanwhile was strongly supported over the exponential model ($\log_{10}$ Bayes factors of 4.4). In addition, it is important to note that among the six Liaoning sequences, only one patient reported having acquired the infection in Liaoning while other patients referred to Guangdong or Sichuan provinces as the likely location of HIV infection, mainly through intravenous drug use. The evidence, therefore, suggests that CRF07_BC sequences from Xinjiang, Liaoning, Guangdong, and Sichuan can probably be traced to a common origin in Yunnan province, a similar pattern to that observed for the CRF08_BC sequences from different regions.

Maximum clade credibility trees revealed that the *env* sequences of subtype C (from India, China, and Myanmar) and of CRF08_BC, CRF07_BC, and other subtype C-related recombinants from China were intermingled in a single cluster, indicating a shared common ancestry, with subtype C strains of Indian origin as outgroup founder strains (Fig. 1c). Coalescence analyses of the *gag-pol* and *env* genes dated the tMRCA of subtype C strains from India and Myanmar to around the mid- to late 1970s (Table 2). Analysis of 14 *env* sequences suggests that subtype C spread into neighboring China later, in 1981.2 (95% CR, 1976.7 to 1985.9), most likely in Yunnan province. Together, the phylogenetic and coalescent results map the eastward movement of subtype C from India to China, probably through Myanmar (2), between the mid-1970s and early 1980s. Finally, the time of origin of the global HIV-1 subtype C was dated 1967.6 (95% CR, 1962.5 to 1972.0) and was highly consistent with previous estimates (44).

To evaluate the possible effects of intrasubtype recombination on the tMRCA estimates, we considered a multilocus model (16) that assumes different genealogies for each locus of the unlinked *gag-pol* data set. BEAST analyses revealed that the tree topologies (figures not shown) and the estimated tMRCAs for the unlinked loci were not significantly different from those of the linked *gag-pol* locus among the overlapping 95% CRs for each locus, especially in those states with younger tMRCAs (Fig. 2). The results suggest that intrasubtype recombination within HIV-1 subtype C and CRF08_BC may not have significant biases on the MRCA dates (16).

DISCUSSION

To our knowledge, this is the first genealogy-based population genetic study of the divergence times of HIV-1 CRF08_BC and CRF07_BC across China. CRF08_BC and CRF07_BC are two subtype C-related recombinants with significant epidemic impact in China and beyond (42, 43). Prior to the emergence of CRF08_BC and CRF07_BC (26, 38), subtype C isolates closely related to Indian strains predominated, especially in the southern part of China (19). Later, subtype C recombined with subtype B′ (10, 45, 47) to form these recombinants. Both recombinants, long thought to have originated from a common birthplace in Yunnan province (20, 49), later dispersed to other areas primarily through drug use and trafficking activities (2). The present study provides new information on the evolutionary and epidemiological characteristics of HIV-1 by establishing the plausible dates of origin and geographic migration patterns of CRF08_BC and CRF07_BC across China. Although the early Indian subtype C strains play no major role in today's epidemic in China, the date of introduction of subtype C into China helps to provide a more complete pict[illegible]e epidemic history of subtype C and its related recombinants in East Asia (Fig. 3).

The Bayesian coalescence analyses show that CRF08_BC emerged in Yunnan province of China in the early 1990s. The virus then spread eastward to neighboring Guangxi (in Baise city near the Yunnan-Guangxi border) in the mid-1990s; this is consistent with historical accounts of CRF08_BC among IDU in this region (24). Inside Guangxi, highly homogeneous CRF08_BC strains from Baise (26, 52) were multiply introduced into Binyang county in 1996 to 1999 and are predominant among IDU (15). Moreover, the relatively recent introduction of CRF08_BC into Pingxiang in the late 1990s estimated here suggests a southward distribution of CRF08_BC near the China-Vietnam border, although CRF01_AE strains closely related to strains of northern Vietnam account for the majority of IDU infections in this region (13, 15). It is also interesting that the CRF08_BC epidemic in Liaoning province, a geographically remote area with low HIV prevalence located in northeastern China, started at almost the same time as that in Guangxi. Our results imply a rapid and simultaneous expansion of CRF08_BC from a common origin in Yunnan to Guangxi and as far as Liaoning province. Although a general trend of migration has been observed, it is essential

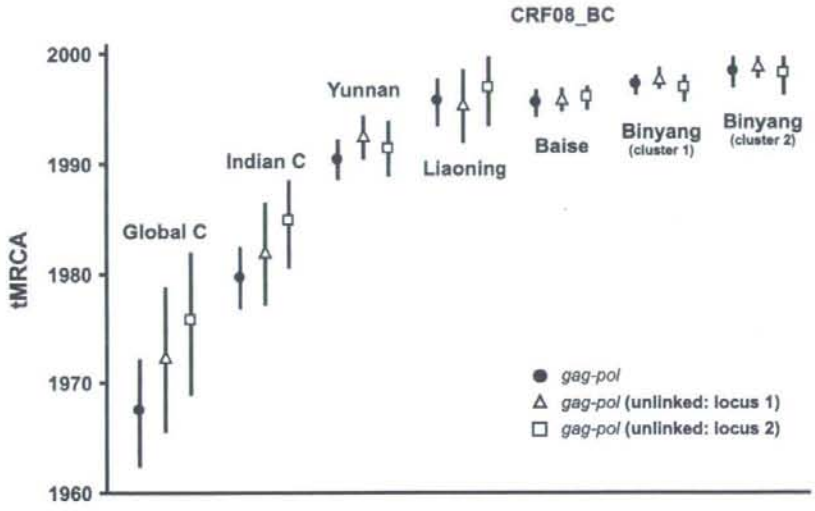

FIG. 2. Dates of the MRCA of HIV-1 subtype C and CRF08_BC estimated in a multiple unlinked locus model. The *gag-pol* gene was partitioned (locus 1 and 2), and Bayesian estimation for each locus was performed in BEAST, assuming a shared demographic history among all loci. The mean coalescence time estimates with 95% highest posterior density for HIV subtype C and CRF08_BC from various geographical origins are illustrated.

to stress that the estimated dates—which merely imply the coalescence times of select viral strains—might not accurately reflect the actual time of CRF08_BC spread in a given region, especially when the sampled population clusters are small. Until more archival specimens are retrieved and thoroughly studied, the complex temporal movement of CRF08_BC lineages (and also other subtypes/CRFs) must be interpreted with discretion.

Phylogenetic reconstruction and coalescence inference show that the CRF07_BC isolates from different mainland Chinese regions (including Xinjiang, Liaoning, and probably Guangdong and Sichuan) most likely share a common ancestor that existed in 1993 in Yunnan province (20, 49). However, it is noteworthy that a single CRF07_BC sequence and a unique B'/C recombinant sequence were located at the base of the *env* maximum-likelihood tree, along with Indian subtype C sequences. This could be explained by two possibilities: (i) there is a recombination breakpoint within the region studied that rendered the phylogenetic inference inaccurate, or (ii) this is a new recombinant that has acquired an Indian subtype C *env* gene. Since no recombination breakpoint is identified within this region, it is likely that a recombination event in the *env* gene involving CRF07_BC and a "founder" Indian C lineage has occurred before the sequence was sampled (where the putative recombination breakpoints are probably located outside the studied region), a phenomenon which is not uncommon (49). Similar explanations also can be applied for the few CRF08_BC sequences that grouped outside the monophyletic cluster in the *env* region.

We previously investigated the spatiotemporal spread of CRF07_BC in Taiwan using *env* gene sequences (43). CRF07_BC was first introduced into southern Taiwan in the late 1990s, most probably from southwestern China (18), and later spread to the central-northern part of Taiwan in the early 2000s, resulting in the largest-ever HIV epidemic in Taiwan, mostly affecting IDU populations. Adding these results to our new analyses performed here, we have retraced the expansive migration of HIV-1 CRF07_BC from its origin in Yunnan to (a) Xinjiang by the north-westward drug trafficking paths, (b) to Liaoning either by direct introduction from Yunnan or through Guangdong/Sichuan, and (c) to Taiwan, possibly through southeastern China via drug trafficking routes.

Recombination is common in HIV infection (31) and serves as one of the intrinsic evolutionary mechanisms that shape the complex HIV diversity. Besides intersubtype recombination, recombination involving closely related lineages of the same subtype within a single individual has been reported (25, 34, 36), leading to possible quantitative discrepancies on linkage disequilibrium, including the loss of phylogenetic correlation between different loci and biases in the genealogical characteristics (i.e., overestimation of the tMRCA) along the HIV genome (35, 46). Our study, however, showed that intrasubtype recombination has no significant impact on the estimated coalescence dates (Fig. 2)—a feature previously observed in HIV-1 group O (16). This could possibly be explained by the high growth rates of HIV-1, as characterized by its star-like population phylogeny (29) where the terminal branches form a substantial proportion of a tree. In the rapidly growing HIV-1 population, recombination events are more likely to affect the terminal branches by increasing the variance in mutation rates rather than biasing the tree topology (16, 21). Consequently, intrasubtype recombination, despite occurring at high frequency, may not significantly influence the divergence times of HIV.

The currently adopted HIV-1 nomenclature guidelines classify HIV-1 CRFs sequentially, according to the first described

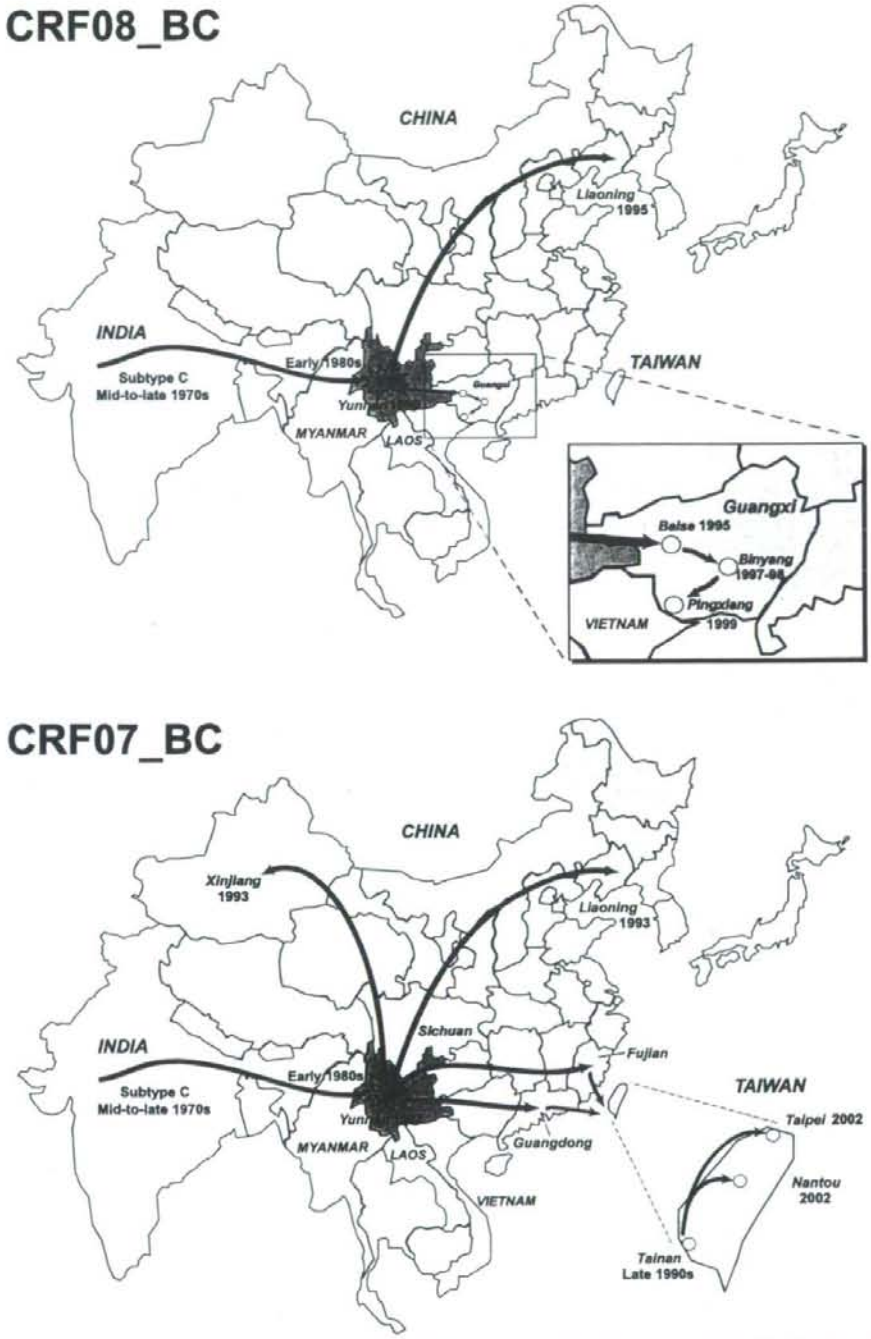

FIG. 3. Plausible site of origin and migration routes of HIV-1 CRF08_BC and CRF07_BC. HIV-1 subtype C of Indian origin entered the Yunnan province (darker shade) in southern China in the early 1980s, possibly via Myanmar. Cocirculation of subtype C and the endemic subtype B′ (10, 45) led to genetic recombination and the generation of CRF08_BC (26) and CRF07_BC (38), two related but distinct B′/C recombinants in Yunnan. Further spread of CRF08_BC and CRF07_BC into other regions in the 1990s mainly through injection drug use (2) has been implicated as the major force spurring the HIV/AIDS epidemic in China. The tMRCAs of CRF08_BC, CRF07_BC, and subtype C strains representing different geographical locations are summarized in Table 2.

full-length or nearly full-length genetic sequences obtained (30), without taking into account the evolutionary history of the viruses (1). Our studies of all available CRF08_BC and CRF07_BC sequences with known sampling dates have shown that CRF08_BC has an earlier evolutionary history than CRF07_BC, which is not readily indicated by the current naming system. We show that CRF08_BC was probably generated approximately 10 years after subtype C of Indian origin was first introduced to Yunnan province, around 1981. CRF07_BC was formed in the same province a few years later, around 1993. The findings highlight the feasibility and relevance of incorporating evolutionary population biology into HIV-1 classification to better reflect the evolutionary pathways of the viruses, particularly for those recombinants with close phylogenetic, genealogical and geographical links (4, 37).

Here, we reconstruct the epidemic histories of HIV-1 CRF08_BC, CRF07_BC and related sequences, inside and beyond China. Injection drug use remains a major transmission mode for HIV-1 CRF08_BC and CRF07_BC throughout China. Phylodynamic investigations are therefore important in unifying the epidemiological and evolutionary dynamics of the highly divergent and rapidly expanding HIV-1 subtypes and CRFs in Asia and elsewhere.

ACKNOWLEDGMENTS

The authors gratefully acknowledge Philippe Lemey and Chung-Chau Hon for assistance, Naoki Yamamoto for support, and Timothy D. Mastro for critical reading of the manuscript. We also thank the anonymous reviewers for their insightful comments.

This study was supported in part by grants from the Ministry of Health, Labour and Welfare (H18-AIDS-General-016); Ministry of Education, Culture, Sports, Science and Technology (Overseas Research Fund); the Japanese Foundation for AIDS Prevention (JFAP) to Y.T.; the Ministry of Science, Technology and Innovation (eScienceFund 02-01-03-SF0379) to A.K.; and the Royal Society University Research Fellowship to O.G.P. and Y.T. K.K.T. is a recipient of the JFAP research resident fellowship.

REFERENCES

1. **Abecasis, A. B., P. Lemey, N. Vidal, T. de Oliveira, M. Peeters, R. Camacho, B. Shapiro, A. Rambaut, and A. M. Vandamme.** 2007. Recombination confounds the early evolutionary history of human immunodeficiency virus type 1: subtype G is a circulating recombinant form. J. Virol. **81**:8543–8551.
2. **Beyrer, C., M. H. Razak, K. Lisam, J. Chen, W. Lui, and X. F. Yu.** 2000. Overland heroin trafficking routes and HIV-1 spread in South and South-East Asia. AIDS **14**:75–83.
3. **Cheng, H., J. Zhang, J. Capizzi, N. L. Young, and T. D. Mastro.** 1994. HIV-1 subtype E in Yunnan, China. Lancet **344**:953–954.
4. **De Sa Filho, D. J., M. C. Sucupira, M. M. Caseiro, E. C. Sabino, R. S. Diaz, and L. M. Janini.** 2006. Identification of two HIV type 1 circulating recombinant forms in Brazil. AIDS Res. Hum. Retrovir. **22**:1–13.
5. **Drummond, A. J., S. Y. Ho, M. J. Phillips, and A. Rambaut.** 2006. Relaxed phylogenetics and dating with confidence. PLoS Biol. **4**:e88.
6. **Drummond, A. J., G. K. Nicholls, A. G. Rodrigo, and W. Solomon.** 2002. Estimating mutation parameters, population history and genealogy simultaneously from temporally spaced sequence data. Genetics **161**:1307–1320.
7. **Drummond, A. J., and A. Rambaut.** 2007. BEAST: Bayesian evolutionary analysis by sampling trees. BMC Evol. Biol. **7**:214.
8. **Gifford, R. J., T. de Oliveira, A. Rambaut, O. G. Pybus, D. Dunn, A. M. Vandamme, P. Kellam, and D. Pillay.** 2007. Phylogenetic surveillance of viral genetic diversity and the evolving molecular epidemiology of human immunodeficiency virus type 1. J. Virol. **81**:13050–13056.
9. **Gilbert, M. T., A. Rambaut, G. Wlasiuk, T. J. Spira, A. E. Pitchenik, and M. Worobey.** 2007. The emergence of HIV/AIDS in the Americas and beyond. Proc. Natl. Acad. Sci. USA **104**:18566–18570.
10. **Graf, M., Y. Shao, Q. Zhao, T. Seidl, J. Kostler, H. Wolf, and R. Wagner.** 1998. Cloning and characterization of a virtually full-length HIV type 1 genome from a subtype B'-Thai strain representing the most prevalent B-clade isolate in China. AIDS Res. Hum. Retrovir. **14**:285–288.
11. **Han, X., M. Zhang, D. Dai, Y. Wang, Z. Zhang, J. Liu, W. Geng, Y. Jiang, Y. Takebe, and H. Shang.** 2007. Genotypic resistance mutations to antiretroviral drugs in treatment-naive HIV/AIDS patients living in Liaoning Province, China: baseline prevalence and subtype-specific difference. AIDS Res. Hum. Retrovir. **23**:357–364.
12. **Hasegawa, M., H. Kishino, and T. Yano.** 1985. Dating of the human-ape splitting by a molecular clock of mitochondrial DNA. J. Mol. Evol. **22**:160–174.
13. **Kato, K., T. Shiino, S. Kusagawa, H. Sato, K. Nohtomi, K. Shibamura, T. H. Nguyen, K. C. Pham, X. L. Truong, H. A. Mai, T. L. Hoang, G. Bunyaraksyotin, Y. Fukushima, M. Honda, C. Wasi, S. Yamazaki, Y. Nagai, and Y. Takebe.** 1999. Genetic similarity of HIV type 1 subtype E in a recent outbreak among injecting drug users in northern Vietnam to strains in Guangxi Province of southern China. AIDS Res. Hum. Retrovir. **15**:1157–1168.
14. **Kingman, J. F. C.** 1982. The coalescent. Stochastic Processes Appl. **13**:235–248.
15. **Laeyendecker, O., G. W. Zhang, T. C. Quinn, R. Garten, S. C. Ray, S. Lai, W. Liu, J. Chen, and X. F. Yu.** 2005. Molecular epidemiology of HIV-1 subtypes in southern China. J. Acquir. Immune Defic. Syndr. **38**:356–362.
16. **Lemey, P., O. G. Pybus, A. Rambaut, A. J. Drummond, D. L. Robertson, P. Roques, M. Worobey, and A. M. Vandamme.** 2004. The molecular population genetics of HIV-1 group O. Genetics **167**:1059–1068.
17. **Li, X. J., S. Kusagawa, X. Xia, C. Yang, Q. Wang, Y. Yokota, Y. Hoshina, T. Onogi, K. Nohtomi, Y. Imamura, T. Shiino, R. Yang, N. Yamamoto, K. Ben, and Y. Takebe.** 2005. Molecular epidemiology of the heterosexual HIV-1 transmission in Kunming, Yunnan Province of China suggests origin from the local IDU epidemic. AIDS Res. Hum. Retrovir. **21**:977–980.
18. **Lin, H. H., Y. L. Shih, Y. C. Liu, S. S. Lee, C. K. Huang, Y. L. Chen, C. Chin, C. H. Lai, H. C. Tsai, Y. C. Guo, and L. Zhang.** 2006. An epidemic of HIV type I CRFU7_BC infection among injection drug users in Taiwan. J. Acquir. Immune Defic. Syndr. **42**:248–255.
19. **Luo, C. C., C. Tian, D. J. Hu, M. Kai, T. Dondero, and X. Zheng.** 1995. HIV-1 subtype C in China. Lancet **345**:1051–1052.
20. **McClutchan, F. E., J. K. Carr, D. Murphy, S. Piyasirisilp, F. Gao, B. Hahn, X. F. Yu, C. Beyrer, and D. L. Birx.** 2002. Precise mapping of recombination breakpoints suggests a common parent of two BC recombinant HIV type 1 strains circulating in China. AIDS Res. Hum. Retrovir. **18**:1135–1140.
21. **McVean, G. A.** 2002. A genealogical interpretation of linkage disequilibrium. Genetics **162**:987–991.
22. **Meng, Z., H. Xing, X. He, L. Ma, W. Xu, and Y. Shao.** 2007. Genetic characterization of three newly isolated CRF07_BC near full-length genomes in China. AIDS Res. Hum. Retrovir. **23**:1049–1054.
23. **Ministry of Health, People's Republic of China, Joint United Nations Programme on HIV/AIDs, and the World Health Organization.** 2006. 2005 Update on the HIV/AIDS epidemic and response in China. National Center for AIDS/STD Prevention and Control, China CDC, Beijing, People's Republic of China.
24. **Ministry of Health, People's Republic of China, and United Nations Theme Group on HIV/AIDS in China.** 1997. China responds to AIDS: HIV/AIDS situation and needs assessment report. Chinese Ministry of Health, Beijing, People's Republic of China.
25. **Philpott, S., H. Burger, C. Tsoukas, B. Foley, K. Anastos, C. Kitchen, and B. Weiser.** 2005. Human immunodeficiency virus type 1 genomic RNA sequences in the female genital tract and blood: compartmentalization and intrapatient recombination. J. Virol. **79**:353–363.
26. **Piyasirisilp, S., F. E. McCutchan, J. K. Carr, E. Sanders-Buell, W. Liu, J. Chen, R. Wagner, H. Wolf, Y. Shao, S. Lai, C. Beyrer, and X. F. Yu.** 2000. A recent outbreak of human immunodeficiency virus type 1 infection in southern China was initiated by two highly homogeneous, geographically separated strains, circulating recombinant form AE and a novel BC recombinant. J. Virol. **74**:11286–11295.
27. **Pybus, O. G., A. J. Drummond, T. Nakano, B. H. Robertson, and A. Rambaut.** 2003. The epidemiology and iatrogenic transmission of hepatitis C virus in Egypt: a Bayesian coalescent approach. Mol. Biol. Evol. **20**:381–387.
28. **Rambaut, A., and A. J. Drummond.** 2007. Tracer v1.4. Institute of Evolutionary Biology, University of Edinburgh, Edinburgh, Scotland. http://tree.bio.ed.ac.uk.
29. **Robbins, K. E., P. Lemey, O. G. Pybus, H. W. Jaffe, A. S. Youngpairoj, T. M. Brown, M. Salemi, A. M. Vandamme, and M. L. Kalish.** 2003. U.S. Human immunodeficiency virus type 1 epidemic: date of origin, population history, and characterization of early strains. J. Virol. **77**:6359–6366.
30. **Robertson, D. L., J. P. Anderson, J. A. Bradac, J. K. Carr, B. Foley, R. K. Funkhouser, F. Gao, B. H. Hahn, M. L. Kalish, C. Kuiken, G. H. Learn, T. Leitner, F. McCutchan, S. Osmanov, M. Peeters, D. Pieniazek, M. Salminen, P. M. Sharp, S. Wolinsky, and B. Korber.** 2000. HIV-1 nomenclature proposal. Science **288**:55–56.
31. **Robertson, D. L., B. H. Hahn, and P. M. Sharp.** 1995. Recombination in AIDS viruses. J. Mol. Evol. **40**:249–259.
32. **Rodenburg, C. M., Y. Li, S. A. Trask, Y. Chen, J. Decker, D. L. Robertson, M. L. Kalish, G. M. Shaw, S. Allen, B. H. Hahn, and F. Gao.** 2001. Near full-length clones and reference sequences for subtype C isolates of HIV type 1 from three different continents. AIDS Res. Hum. Retrovir. **17**:161–168.

33. **Rodriguez, F., J. L. Oliver, A. Marin, and J. R. Medina.** 1990. The general stochastic model of nucleotide substitution. J. Theor. Biol. **142**:485–501.
34. **Rousseau, C. M., G. H. Learn, T. Bhattacharya, D. C. Nickle, D. Heckerman, S. Chetty, C. Brander, P. J. Goulder, B. D. Walker, P. Kiepiela, B. T. Korber, and J. I. Mullins.** 2007. Extensive intrasubtype recombination in South African human immunodeficiency virus type 1 subtype C infections. J. Virol. **81**:4492–4500.
35. **Schierup, M. H., and J. Hein.** 2000. Consequences of recombination on traditional phylogenetic analysis. Genetics **156**:879–891.
36. **Shriner, D., A. G. Rodrigo, D. C. Nickle, and J. I. Mullins.** 2004. Pervasive genomic recombination of HIV-1 in vivo. Genetics **167**:1573–1583.
37. **Sierra, M., M. M. Thomson, D. Posada, L. Perez, C. Aragones, Z. Gonzalez, J. Perez, G. Casado, and R. Najera.** 2007. Identification of 3 phylogenetically related HIV-1 BG intersubtype circulating recombinant forms in Cuba. J. Acquir. Immune Defic. Syndr. **45**:151–160.
38. **Su, L., M. Graf, Y. Zhang, H. von Briesen, H. Xing, J. Kostler, H. Melzl, H. Wolf, Y. Shao, and R. Wagner.** 2000. Characterization of a virtually full-length human immunodeficiency virus type 1 genome of a prevalent intersubtype (C/B′) recombinant strain in China. J. Virol. **74**:11367–11376.
39. **Suchard, M. A., R. E. Weiss, and J. S. Sinsheimer.** 2001. Bayesian selection of continuous-time Markov chain evolutionary models. Mol. Biol. Evol. **18**:1001–1013.
40. **Swofford, D. L.** 2003. PAUP*, phylogenetic analysis using parsimony (*and other methods), 4.0 beta ed. Sinauer Associates, Sunderland, MA.
41. **Takebe, Y., K. Motomura, M. Tatsumi, H. H. Lwin, M. Zaw, and S. Kusagawa.** 2003. High prevalence of diverse forms of HIV-1 intersubtype recombinants in central Myanmar: geographical hot spot of extensive recombination. AIDS **17**:2077–2087.
42. **Tebit, D. M., I. Nankya, E. J. Arts, and Y. Gao.** 2007. HIV diversity, recombination and disease progression: how does fitness "fit" into the puzzle? AIDS Rev. **9**:75–87.
43. **Tee, K. K., O. G. Pybus, H. Liao, R. Uenishi, S. Hase, A. Kamarulzaman, X. J. Li, and Y. Takebe.** 2008. Chronology of the HIV-1 CRF07_BC expansion in East Asia. AIDS **22**:156–158.
44. **Travers, S. A., J. P. Clewley, J. R. Glynn, P. E. Fine, A. C. Crampin, F. Sibande, D. Mulawa, J. O. McInerney, and G. P. McCormack.** 2004. Timing and reconstruction of the most recent common ancestor of the subtype C clade of human immunodeficiency virus type 1. J. Virol. **78**:10501–10506.
45. **Weniger, B. G., Y. Takebe, C. Y. Ou, and S. Yamazaki.** 1994. The molecular epidemiology of HIV in Asia. AIDS **8**(Suppl. 2):S13–S28.
46. **Worobey, M.** 2001. A novel approach to detecting and measuring recombination: new insights into evolution in viruses, bacteria, and mitochondria. Mol. Biol. Evol. **18**:1425–1434.
47. **Xia, M., J. K. Kreiss, and K. K. Holmes.** 1994. Risk factors for HIV infection among drug users in Yunnan province, China: association with intravenous drug use and protective effect of boiling reusable needles and syringes. AIDS **8**:1701–1706.
48. **Yang, R., S. Kusagawa, C. Zhang, X. Xia, K. Ben, and Y. Takebe.** 2003. Identification and characterization of a new class of human immunodeficiency virus type 1 recombinants comprised of two circulating recombinant forms, CRF07_BC and CRF08_BC, in China. J. Virol. **77**:685–695.
49. **Yang, R., X. Xia, S. Kusagawa, C. Zhang, K. Ben, and Y. Takebe.** 2002. On-going generation of multiple forms of HIV-1 intersubtype recombinants in the Yunnan Province of China. AIDS **16**:1401–1407.
50. **Yang, Z.** 1994. Maximum likelihood phylogenetic estimation from DNA sequences with variable rates over sites: approximate methods. J. Mol. Evol. **39**:306–314.
51. **Yu, X. F., J. Chen, Y. Shao, C. Beyrer, and S. Lai.** 1998. Two subtypes of HIV-1 among injection-drug users in southern China. Lancet **351**:1250.
52. **Yu, X. F., W. Liu, J. Chen, W. Kong, B. Liu, Q. Zhu, F. Liang, F. McCutchan, S. Piyasirisilp, and S. Lai.** 2002. Maintaining low HIV type 1 env genetic diversity among injection drug users infected with a B/C recombinant and CRF01_AE HIV type 1 in southern China. AIDS Res. Hum Retrovir. **18**:167–170.
53. **Zheng, X., C. Tian, K. H. Choi, J. Zhang, H. Cheng, X. Yang, D. Li, J. Lin, S. Qu, X. Sun, T. Hall, J. Mandel, and N. Hearst.** 1994. Injecting drug use and HIV infection in southwest China. AIDS **8**:1141–1147.

Research Letters

AIDS 2008, **22**:1081–1089

Cyclin K/CPR4 inhibits primate lentiviral replication by inactivating Tat/positive transcription elongation factor b-dependent long terminal repeat transcription

Emiko Urano[a,b], Saki Shimizu[a], Yuko Futahashi[a], Makiko Hamatake[a], Yuko Morikawa[b], Naoko Takahashi[c], Hidesuke Fukazawa[c], Naoki Yamamoto[a] and Jun Komano[a]

The positive transcription elongation factor b complexes comprise CDK9 and a C-type cyclin, required for the efficient expression of both eukaryotic and primate lentivirus-encoded genes. Cyclin K/CPR4 is the least studied of the positive transcription elongation factor b-forming cyclins. Here, we demonstrate that cyclin K/CPR4-containing positive transcription elongation factor b complexes are unresponsive to Tat and HEXIM1-mediated inactivation. Enhancing expression of cyclin K/CPR4 inhibited the human and simian immunodeficiency viral replication. These data indicate that cyclin K/CPR4 functions as a natural inhibitor of primate lentiviruses.

Positive transcription elongation factor b (P-TEFb) complexes comprise CDK9 and a C-type cyclin (cyclin T1, T2 or K) and play a role in transcriptional initiation in/or elongation of cellular genes [1–6]. The P-TEFb complex is critical for Tat-dependent transcription from the human and simian immunodeficiency virus (HIV-1 and SIV) long terminal repeat (LTR) promoter. By interacting with the P-TEFb complex, Tat recruits the P-TEFb complex to the trans-activation-responsive (TAR) viral RNA element, which is located close to the transcriptional start site to which Tat binds in complex with P-TEFb complex. CDK9 phosphorylates the carboxy-terminal domain of RNA polymerase II, which boosts transcription from the proviral genome [7]. Among the P-TEFb complex-forming cyclins, only CCNT1 has the Tat responsive motif (TRM). Given the structural and functional similarities between CCNT2 and CCNK [8], expression of CCNK has been assumed to negatively affect Tat-dependent transcription, thus primate lentiviral replication. This possibility, however, has not yet been examined. Recently, it was found that the P-TEFb complex containing CCNT1 or CCNT2 is inactivated by the 7SK RNA–HEXIM1 complex [9–12]. The HEXIM1-mediated inhibition of CCNK-containing P-TEFb complexes remains to be tested.

We constructed mammalian expression plasmids for wild type and N-terminal FLAG-tagged or green fluorescent protein (GFP)-tagged human CCNK (WT, fCCNK or GFP-fCCNK). The CCNK function is unaffected by N-terminal epitope tagging [2,13,14]. GFP-fCCNK was used to examine the intracellular localization of fCCNK in NP2 cells. GFP-fCCNK accumulated in the discrete nuclear speckle compartments, similar to GFP-CCNT1, known to be sites of RNA Pol II-mediated transcription and co-transcriptional premRNA processing [15] and exhibited co-distribution with hemaglutinin eipope tagged CDK9 (data not shown). These data suggest functional similarities between CCNK and CCNT1.

We examined the physical association between CCNK and the transcriptional regulators HEXIM1 and HIV-1 Tat. Under the same conditions, endogenously expressed HEXIM1 did not co-immunoprecipitate with fCCNK, but co-immunoprecipitated successfully with FLAG-tagged CCNT1 (fCCNT1; Fig. 1a). Similarly, FLAG-tagged Tat could not co-immunoprecipitate CCNK under conditions in which it did precipitate GFP-CCNT1 (Fig. 1a). These data suggest that the CCNK-containing P-TEFb complex is unresponsive to HEXIM1 or Tat and, thus, it would appear that CCNK is unique among P-TEFb complex-forming cyclins.

To test whether CCNK expression reduces HIV-1 production at the level of transcription, we performed a transient transfection assay to measure HIV-1 production in the presence of different levels of CCNK expression. HIV-1 proviral DNA was co-introduced into 293 T cells with increasing amounts of fCCNK expression plasmid. It was found that the viral production was decreased dramatically in a dose-dependent manner (Fig. 1b). Similarly, the production of SIV was reduced (data not shown). Western blot analysis revealed that the level of p24 antigen in cell lysates dropped significantly with increasing levels of fCCNK (Fig. 1b). By contrast, the level of the internal control Bip was unaffected (Fig. 1b). Real-time (RT)-PCR analysis revealed that viral mRNA levels fell with increasing fCCNK expression, whereas the internal control cyclophilin A mRNA levels were unaffected (Fig. 1b). The reduction in viral mRNA was comparable with that observed for viral protein. Specifically, RT-PCR demonstrated that 80 ng of pfCCNK exerted the maximum reduction in viral mRNA levels (5.1% relative to the control), a finding similar to the viral production levels quantified by enzyme-linked immunosorbent assay (3.3%, Fig. 1b). These data strongly suggest that CCNK inhibits HIV-1

ISSN 0269-9370

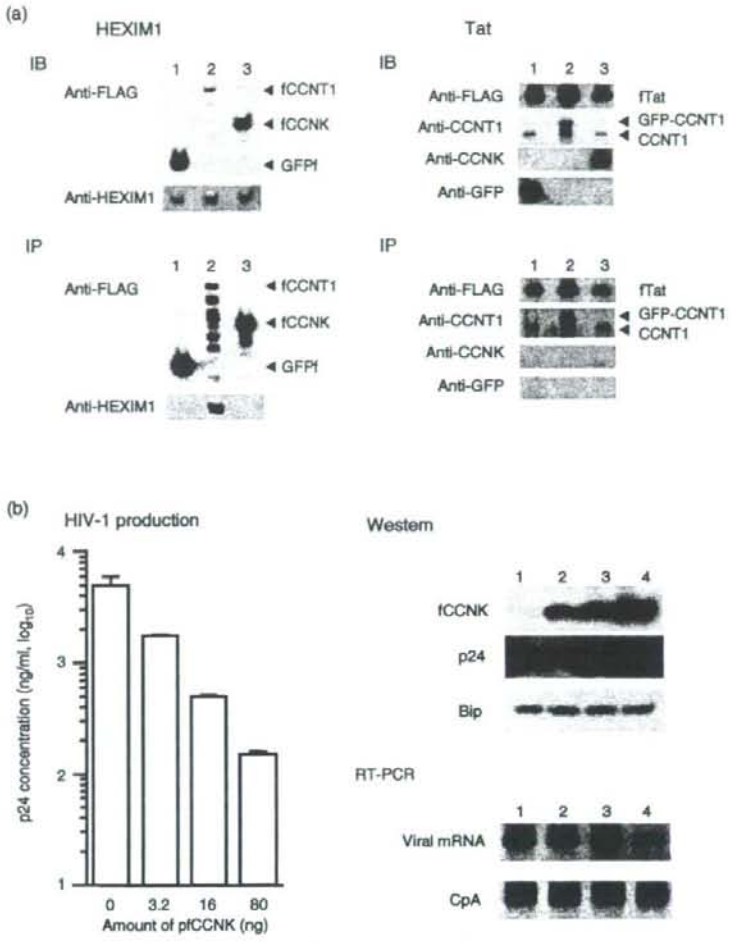

Fig. 1. Expression and functional characterization of cyclin K/CPR4. (a) Co-immunoprecipitation assay demonstrating that cyclin K/CPR4 does not interact with HEXIM1 or HIV-1 Tat. For the co-immunoprecipitation assay with HEXIM1, 293 T cells were transfected with 2 μg of expression vector and then grown in six-well plates. Expression vectors included FLAG-tagged green fluorescent protein (GFP) (lane 1, GFPf), FLAG-tagged CCNT1 (lane 2, fCCNT1) and FLAG-tagged cyclin K/CPR4 (lane 3, fCCNK). For the co-immunoprecipitation assay with Tat, 293 T cells were co-transfected with 1 μg FLAG-tagged Tat (fTat) and 1 μg of GFP (lane 1), GFP-CCNT1 (lane 2) or cyclin K/CPR4 (lane 3). Protein expressions from transfected plasmids were detected by western blot analysis (IB). Cell lysates were immunoprecipitated with agarose beads conjugated with anti-FLAG M2 antibody. Co-immunoprecipitated proteins were separated by SDS-PAGE and immunoblotted using the antibodies indicated (IP). (b) fCCNK expression inhibited transcription of HIV-1. The 293 T cells were co-transfected with HIV-1 proviral DNA (200 ng) and increasing amounts of the fCCNK expression plasmid (0, 3.2, 16 and 80 ng per well in a six-well plate). Viral production was examined 48 h post-transfection by p24 enzyme-linked immunosorbent assay. Western blot analysis was used to examine expression levels of fCCNK, p24 antigen and Bip in transfected 293 T cells. Real-time polymerase chain reaction was used to examine viral and cyclophilin A mRNA expression in transfected 293 T cells. Lanes 1–4 correspond to the amount of pfCCNK 0, 3.2, 16, and 80 ng, respectively.

production by specifically limiting Tat-dependent LTR transcription.

Finally, we investigated the potential inhibitory activity of CCNK on HIV-1 replication in a physiologically relevant system. We established human T cell lines that constitutively overexpressed fCCNK or luciferase (Luc) by infecting MOLT-4, MT-4 and M8166 cells with murine leukemia viral vectors carrying fCCNK-IRES-GFP or Luc-IRES-GFP cassettes and GFP-positive cells were collected as described previously to examine the role of HEXIM1 in the primate lentiviral replication [16]. Expression of fCCNK was verified by western blot analysis using an anti-CCNK antibody and the expression

of cellular proteins such as CCNT1, CDK9, HEXIM1, Bip, and cell surface receptors for HIV-1 (CD4 and CXCR4) was comparable between fCCNK-expressing and Luc-expressing cells. In addition, no differences in rate of cell proliferation were detected between fCCNK-expressing and Luc-expressing cells (data not shown). We measured HIV-1 and SIV replication in these T cell lines and found that the viral replication was strongly inhibited in all the three fCCNK-expressing T cell lines (data not shown). These data directly demonstrate that CCNK functions as a negative regulator of primate lentiviral replication. In addition, we verified that constitutive fCCNK expression did not block the early phase of the viral life cycle by conducting a real-time Alu-LTR PCR assay to quantify the integrated viral genome in MOLT-4 and MT-4 cells infected with VSV-G-pseudotyped replication-incompetent HIV-1 vector (data not shown).

Taken together, our results indicate that CCNK is able to limit the replication of primate lentiviruses by competing with CCNT1 for CDK9, which results in a reduction of CCNT1-containing Tat-responsive P-TEFb complexes, thereby inactivation of Tat/P-TEFb-dependent transcription of the viral LTR promoter. Our report is the first demonstration that constitutive upregulation of a C-type cyclin CCNK limits primate lentiviral replication in human T cell lines without conferring any detectable effect on cell proliferation. The lack of any detectable effect on cell proliferation could be because CCNK-containing P-TEFb complexes can complement the role played by the CCNT1-containing P-TEFb complex in cellular gene transcription. These data highlight the importance of Tat-dependent LTR transcription for the efficient propagation of the primate lentivirus and the potential protective role of CCNK in the pathogenesis of primate lentiviruses.

Acknowledgements

This work was supported in part by the Japan Health Science Foundation, the Japanese Ministry of Health, Labor and Welfare (H18-AIDS-W-003) and the Japanese Ministry of Education, Culture, Sports, Science and Technology (18689014 and 18659136).

[a]*AIDS Research Center, National Institute of Infectious Diseases, Shinjuku-ku, Tokyo;* [b]*Kitasato Institute of Life Sciences, Kitasato University, Minato-ku, Tokyo; and* [c]*Department of Bioactive Molecules, National Institute of Infectious Diseases, 1-23-1, Toyama, Shinjuku-ku, Tokyo, Japan.*

Correspondence to Jun Komano, AIDS Research Center, National Institute of Infectious Diseases, 1-23-1 Toyama, Shinjuku, Tokyo 162-8640, Japan.
Tel: +81 3 5285 1111; fax: +81 3 5285 5037;
e-mail: ajkomano@nih.go.jp

References

1. Peng J, Zhu Y, Milton JT, Price DH. **Identification of multiple cyclin subunits of human P-TEFb.** *Genes Dev* 1998; **12**:755–762.
2. Fu TJ, Peng J, Lee G, Price DH, Flores O. **Cyclin K functions as a CDK9 regulatory subunit and participates in RNA polymerase II transcription.** *J Biol Chem* 1999; **274**:34527–34530.
3. Price DH. **P-TEFb, a cyclin-dependent kinase controlling elongation by RNA polymerase II.** *Mol Cell Biol* 2000; **20**:2629–2634.
4. Garriga J, Grana X. **Cellular control of gene expression by T-type cyclin/CDK9 complexes.** *Gene* 2004; **337**:15–23.
5. Dulac C, Michels A, Fraldi A, Bonnet F, Nguyen Vt, Napolitano GETA. **Transcription-dependent association of multiple positive transcription elongation factor units to a HEXIM multimer.** *J Biol Chem* 2005; **280**:30619–30629.
6. Peterlin BM, Price DH. **Controlling the elongation phase of transcription with P-TEFb.** *Mol Cell* 2006; **23**:297–305.
7. Garber M, Wei P, Jones K. **HIV-1 Tat interacts with cyclin T1 to direct the P-TEFb CTD kinase complex to TAR RNA.** *Cold Spring Harb Symp Quant Biol* 1998; **63**:371–380.
8. Napolitano G, Licciardo P, Gallo P, Majello B, Giordano A, Lania L. **The CDK9-associated cyclins T1 and T2 exert opposite effects on HIV-1 Tat activity.** *AIDS* 1999; **13**:1453–1459.
9. Zhou Q, Yik JH. **The Yin and Yang of P-TEFb regulation: implications for human immunodeficiency virus gene expression and global control of cell growth and differentiation.** *Microbiol Mol Biol Rev* 2006; **70**:646–659.
10. Michels A, Fraldi A, Li Q, Adamson Te, Bonnet F, Nguyen Vt, *et al.* **Binding of the 7SK snRNA turns the HEXIM1 protein into a P-TEFb (CDK9/cyclin T) inhibitor.** *EMBO J* 2004; **23**:2608–2619.
11. Yik J, Chen R, Pezda A, Samford C, Zhou Q. **A human immunodeficiency virus type 1 Tat-like arginine-rich RNA-binding domain is essential for HEXIM1 to inhibit RNA polymerase II transcription through 7SK snRNA-mediated inactivation of P-TEFb.** *Mol Cell Biol* 2004; **24**:5094–5105.
12. Barboric M, Kohoutek J, Price J, Blazek D, Price D, Peterlin B. **Interplay between 7SK snRNA and oppositely charged regions in HEXIM1 direct the inhibition of P-TEFb.** *EMBO J* 2005; **24**:4291–4303.
13. Edwards MC, Wong C, Elledge SJ. **Human cyclin K, a novel RNA polymerase II-associated cyclin possessing both carboxy-terminal domain kinase and Cdk-activating kinase activity.** *Mol Cell Biol* 1998; **18**:4291–4300.
14. Lin X, Taube R, Fujinaga K, Peterlin BM. **P-TEFb containing cyclin K and Cdk9 can activate transcription via RNA.** *J Biol Chem* 2002; **277**:16873–16878; [Epub ahead of print, 1 March 2002].
15. Herrmann CH, Mancini MA. **The Cdk9 and cyclin T subunits of TAK/P-TEFb localize to splicing factor-rich nuclear speckle regions.** *J Cell Sci* 2001; **114**:1491–1503.
16. Shimizu S, Urano E, Futahashi Y, Miyauchi K, Isogai M, Matsuda Z, *et al.* **Inhibiting lentiviral replication by HEXIM1, a cellular negative regulator of the CDK9/cyclin T complex.** *AIDS* 2007; **21**:575–582.

Potential role of CD8+CD28− T lymphocytes in immune activation during HIV-1 infection

Nancy Vivar[a], Pham Hong Thang[a,b], Ann Atlas[c], Francesca Chiodi[a] and Bence Rethi[a,d]

As CD8+CD28− T cells have been associated with dendritic and T cell suppression, we analyzed whether an increase in CD8+CD28− T cell numbers during HIV-1 infection could lead to impaired T cell responses. In contrast to the in-vitro generated CD8+CD28− suppressors, peripheral blood CD8+CD28− T cells of both HIV-infected and

SOCS1 is an inducible host factor during HIV-1 infection and regulates the intracellular trafficking and stability of HIV-1 Gag

Akihide Ryo[a,b,c], Naomi Tsurutani[d], Kenji Ohba[b,e], Ryuichiro Kimura[e,f], Jun Komano[b], Mayuko Nishi[a], Hiromi Soeda[a], Shinichiro Hattori[b], Kilian Perrem[g], Mikio Yamamoto[h], Joe Chiba[f], Jun-ichi Mimaya[i], Kazuhisa Yoshimura[i], Shuzo Matsushita[i], Mitsuo Honda[b], Akihiko Yoshimura[k], Tatsuya Sawasaki[l], Ichiro Aoki[a], Yuko Morikawa[d], and Naoki Yamamoto[b,c]

[a]Department of Pathology, Yokohama City University School of Medicine, 3-9 Fuku-ura, Kanazawa-ku, Yokohama 236-0004, Japan; [b]AIDS Research Center, National Institute of Infectious Diseases, 1-23-1 Toyama, Shinjuku-ku, Tokyo 162-8640, Japan; [d]Kitasato Institute for Life Sciences, Kitasato University, Shirokane 5-9-1, Minato-ku, Tokyo 108-8641, Japan; [e]Department of Molecular Virology, Graduate School of Medicine, Tokyo Medical and Dental University, 1-5-45 Yushima, Bunkyo-ku, Tokyo 113-8519, Japan; [f]Molecular Oncology Laboratory, Department of Pathology, Royal College of Surgeons in Ireland, Smurfit Building, Beaumont Hospital, Dublin 9, Ireland; [h]Department of Biochemistry II, National Defense Medical College, 3-2 Namiki, Tokorozawa-shi, Saitama 359-8513, Japan; [g]Department of Biological Science and Technology, Science University of Tokyo, 2641 Yamazaki, Noda, Chiba 278-8510, Japan; [i]Division of Hematology and Oncology, Shizuoka Children's Hospital, 860 Urushiyama, Aoi-ku, Shizuoka 420-8660, Japan; [j]Division of Clinical Retrovirology and Infectious Diseases, Center for AIDS Research, Graduate School of Medical Sciences, Kumamoto University, Kumamoto 860-0811, Japan; [k]Division of Molecular and Cellular Immunology, Medical Institute of Bioregulation, Kyushu University, Fukuoka 812-8582, Japan; and [l]Cell Free Science and Research Center, Ehime University, Ehime 790-8577, Japan

Edited by Robert C. Gallo, University of Maryland, Baltimore, MD, and approved November 19, 2007 (received for review May 24, 2007)

Human immunodeficiency virus type 1 (HIV-1) utilizes the macromolecular machinery of the infected host cell to produce progeny virus. The discovery of cellular factors that participate in HIV-1 replication pathways has provided further insight into the molecular basis of virus–host cell interactions. Here, we report that the suppressor of cytokine signaling 1 (SOCS1) is an inducible host factor during HIV-1 infection and regulates the late stages of the HIV-1 replication pathway. SOCS1 can directly bind to the matrix and nucleocapsid regions of the HIV-1 p55 Gag polyprotein and enhance its stability and trafficking, resulting in the efficient production of HIV-1 particles via an IFN signaling-independent mechanism. The depletion of SOCS1 by siRNA reduces both the targeted trafficking and assembly of HIV-1 Gag, resulting in its accumulation as perinuclear solid aggregates that are eventually subjected to lysosomal degradation. These results together indicate that SOCS1 is a crucial host factor that regulates the intracellular dynamism of HIV-1 Gag and could therefore be a potential new therapeutic target for AIDS and its related disorders.

AIDS | pathogenesis | drug target | lysozyme

Human immunodeficiency virus type 1 (HIV-1) infection is a multistep and multifactorial process mediated by a complex series of virus–host cell interactions (1, 2). The molecular interactions between host cell factors and HIV-1 are vital to our understanding of not only the nature of the resulting viral replication, but also the subsequent cytopathogenesis that occurs in the infected cells (3). The characterization of the genes in the host cells that are up- or down-regulated upon HIV-1 infection could therefore provide a further elucidation of virus–host cell interactions and identify putative molecular targets for the HIV-1 replication pathway (4).

The HIV-1 p55 Gag protein consists of four domains that are cleaved by the viral protease concomitantly with virus release. This action generates the mature Gag protein comprising the matrix (MA/p17), capsid (CA/p24), nucleocapsid (NC/p7), and p6 domains, in addition to two small spacer peptides, SP1 and SP2 (5, 6). The N-terminal portion of MA, which is myristoylated, facilitates the targeting of Gag to the plasma membrane (PM), whereas CA and NC promote Gag multimerization. p6 plays a central role in the release of HIV-1 particles from PM by interacting with the vacuolar sorting protein Tsg101 and AIP1/ALIX (7–9). Several recent studies have implicated the presence of host factors in the control of the intracellular trafficking of Gag. AP-3δ is a recently characterized endosomal adaptor protein that binds directly to the MA region of Gag and enhances its targeting to the multivesicular body (MVB) during the early stages of particle assembly (10). The *trans*-Golgi network (TGN)-associated protein hPOSH plays another role in Gag transport by facilitating the egress of Gag cargo vesicles from the TGN, where it assembles with envelope protein (Env) before transport to PM (11). Although the involvement of these host proteins in the regulation of intracellular Gag trafficking has been proposed, the detailed molecular mechanisms underlying this process are still not yet well characterized.

In our current work, we demonstrate that the suppressor of cytokine signaling 1 (SOCS1) directly binds HIV-1 Gag and facilitates the intracellular trafficking and stability of this protein, resulting in the efficient production of HIV-1 particles. These results indicate that SOCS1 is a crucial host factor for efficient HIV-1 production and could be an intriguing molecular target for future treatment of AIDS and related diseases.

Results

SOCS1 Is Induced upon HIV-1 Infection and Facilitates HIV-1 Replication via Posttranscriptional Mechanisms. We and others have shown that HIV-1 infection can alter cellular gene expression patterns, resulting in the modification of viral replication and impaired homeostasis in the host cells (4, 12). Hence, to elucidate further the genes and cellular pathways that participate in HIV-1 replication processes, we performed serial analysis of gene expression (SAGE) using either a HIV-1 or mock-infected human T cell line, MOLT-4 (12). Further detailed analysis of relatively low-abundance SAGE tags identified *SOCS1* as a preferentially up-regulated gene after HIV-1 infection. This finding was validated by both semiquantitative RT-PCR and immunoblotting analysis with anti-SOCS1 anti-

Author contributions: A.R. and N.T. contributed equally to this work; A.R., A.Y., Y.M., and N.Y. designed research; A.R., N.T., K.O., R.K., M.N., H.S., S.H., T.S., I.A., and Y.M. performed research; J.K., S.H., M.Y., J.C., J.-i.M., K.Y., S.M., M.H., and A.Y. contributed new reagents/analytic tools; A.R., N.T., K.O., M.N., H.S., K.P., M.Y., K.Y., S.M., T.S., I.A., Y.M., and N.Y. analyzed data; and A.R., K.P., and N.Y. wrote the paper.

The authors declare no conflict of interest.

This article is a PNAS Direct Submission.

Freely available online through the PNAS open access option.

[c]To whom correspondence may be addressed. E-mail: aryo@nih.go.jp or nyama@nih.go.jp.

This article contains supporting information online at www.pnas.org/cgi/content/full/0704831105/DC1.

www.pnas.org/cgi/doi/10.1073/pnas.0704831105

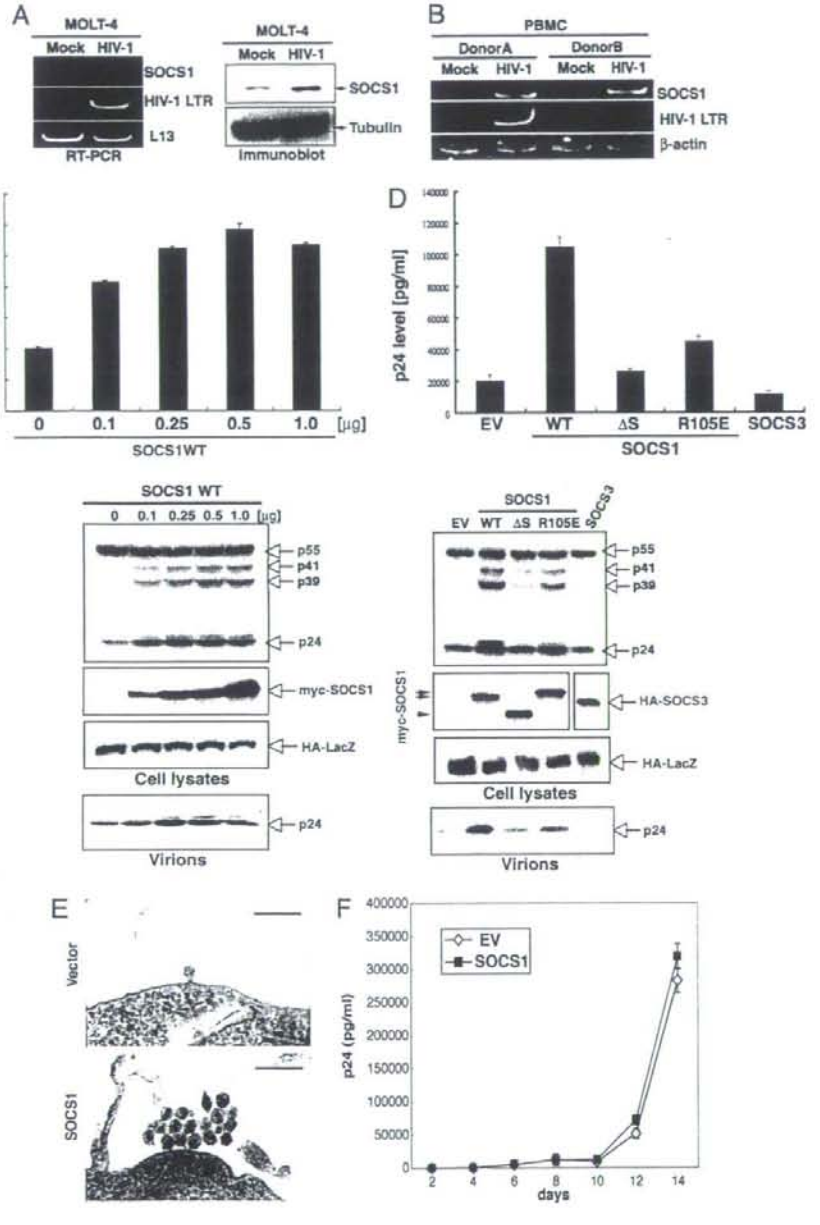

Fig. 1. SOCS1 is induced upon HIV-1 infection and enhances HIV-1 particle production. (*A*) MOLT-4 cells were mock-infected or infected with HIV-1_{NL4-3}, and then total RNA and protein extracts derived from these cells were subjected to semiquantitative RT-PCR (*Left*) and immunoblotting (*Right*), respectively. (*B*) PBMC from two healthy individuals were infected with HIV-1_{NL4-3} or were mock-infected, and SOCS1 expression was examined by semiquantitative RT-PCR. (*C*) 293T cells were transfected with pNL4-3 and cotransfected with various amounts of pcDNA-myc-SOCS1. Forty eight hours after transfection, p24 antigen release into the supernatant in each case was measured by antigen-capture ELISA (*Upper*), and the cell lysates and pelleted viruses were analyzed by immunoblotting (*Lower*). The data shown represent the mean ± SD from three independent experiments. HA-LacZ is a transfection control. (*D*) 293T cells were transfected with pNL4-3 and cotransfected with control vector, SOCS1 (WT), SOCS1ΔS (ΔSOCS box), SOCS1R105E, or SOCS3. Cell lysates and pelleted viruses were then collected after 48 h and subjected to ELISA (*Upper*) or immunoblotting (*Lower*), as described in *C*. (*E*) 293T cells cotransfected with either pNL4-3 plus control vector, or pNL4-3 plus myc-tagged SOCS1 were analyzed by TEM. Note that substantial numbers of mature virus particles can be observed in the myc-SOCS1-transfected cells. (Scale bars: 500 nm.) (*F*) Jurkat cells were infected with virions (adjusted by p24 levels) from either control vector (EV)- or SOCS1-transfected 293T cells. Supernatant p24 levels at the indicated time points were measured by ELISA.

bodies (Fig. 1*A*). In addition, *SOCS1* was found to be up-regulated also in peripheral blood mononuclear cells (PBMC) from two different individuals (following HIV infection, Fig. 1*B*).

Our initial findings that SOCS1 is induced upon HIV-1 infection prompted us to examine whether this gene product affects viral replication. We first cotransfected 293T cells with a HIV-1 infectious molecular clone, pNL4-3 (13), and also pcDNA-myc-SOCS1, and then monitored the virus production levels in the resulting supernatant. We then performed ELISA using an anti-p24 antibody and found that wild-type SOCS1 significantly increases the production of HIV-1 in the cell supernatant in a dose-dependent manner (Fig. 1*C Upper*). In contrast, neither the SH2 domain-defective mutant (R105E) nor the SOCS box deletion mutant (ΔS) of SOCS1 could promote virus production to the same levels as wild type, indicating that both domains are required for this enhancement (Fig. 1*D Upper*). Furthermore, another SOCS box protein, SOCS3, failed to augment HIV-1 replication in a parallel experiment (Fig. 1*D Upper*), indicating that the role of SOCS1 during HIV-1 replication is specific.

We next performed immunoblotting analysis using cell lysates and harvested virus particles in further parallel experiments (Fig. 1 *C* and *D Lower*). Consistent with our ELISA analysis, the expres-

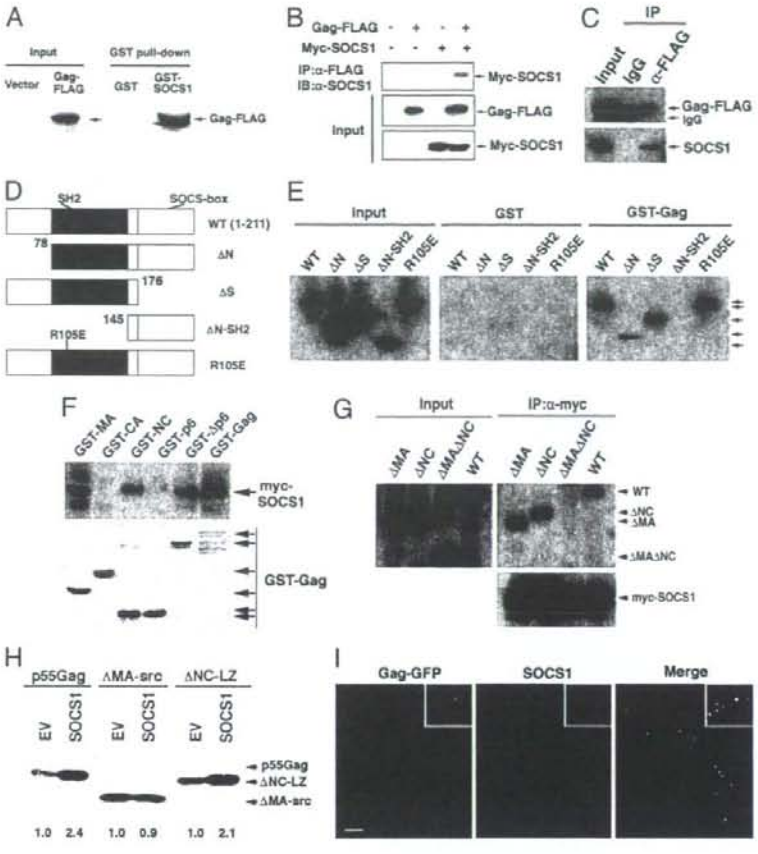

Fig. 2. SOCS1 interacts with HIV-1 Gag. (*A*) Extracts of 293T cells transfected with either empty vector or Gag-FLAG were subjected to pull-down analyses using glutathione–agarose beads with GST-SOCS1 in the presence of 10 ng/ml RNase followed by immunoblotting with anti-FLAG antibodies. (*B*) Extracts of 293T cells transiently expressing myc-SOCS1 and Gag-FLAG were subjected to immunoprecipitation (IP) with anti-FLAG monoclonal antibodies in the presence of 10 ng/ml RNase followed by immunoblotting (IB) analysis with either anti-FLAG or anti-myc polyclonal antibodies. (*C*) 293T cells were transiently transfected with Gag-FLAG, and cell lysates were then subjected to immunoprecipitation with anti-FLAG antibodies followed by immunoblotting with an antibody directed against endogenous SOCS1. (*D* and *E*) 293T cells expressing various myc-tagged SOCS1 mutants (schematically depicted in *D*) were analyzed by GST pull-down analysis with either GST or GST-Gag recombinant protein (*E*). (*F*) GST fusion proteins of the indicated regions of Gag were bound to glutathione beads and incubated with cell lysates from 293T cells expressing myc-SOCS1 in the presence of 10 ng/ml RNase followed by immunoblotting with anti-myc antibodies. (*G*) SOCS1 binds p55 Gag via either its MA or NC domains. 293T cells were transfected with myc-SOCS1 and cotransfected with Gag-FLAG, GagΔMA-FLAG, GagΔNC-FLAG, or GagΔMAΔNC-FLAG. At 24 h after transfection, cell lysates treated with 10 μg/ml RNase were subjected to coimmunoprecipitation with anti-myc monoclonal antibodies followed by immunoblotting with anti-FLAG or anti-myc polyclonal antibodies. (*H*) Functional interaction of SOCS1 with MA but not NC. 293T cells were transfected with wild-type Gag, ΔMA-src, or ΔNC-LZ (Z_{IL}-p6) and cotransfected with either control vector or SOCS1. Supernatant virus particles were then collected after 24 h and subjected to immunoblotting with anti-p24 antibody. Numerical values below the blots indicate fold induction of supernatant p55 signal intensities derived by densitometry. (*I*) Colocalization of SOCS1 with Gag. HeLa cells were transiently transfected with Gag-GFP. After 24 h, the cells were fixed, permeabilized, and immunostained with anti-SOCS1 polyclonal antibody followed by fluorescently labeled secondary antibodies before confocal microscopy. (Scale bar: 10 μm.)

sion of wild-type SOCS1, but neither its SH2 nor SOCS box mutant counterparts, resulted in a marked and dose-dependent increase in the level of intracellular Gag protein, particularly in the case of CA (p24) and intermediate cleavage products corresponding to MA-CA (p41) and CA-NC (p39). This increase was found to be accompanied by an enhanced level of HIV-1 particle production in the supernatant (Fig. 1 *C* and *D Lower*). These results together indicated that SOCS1 facilitates HIV-1 particle production in infected cells and that this role of SOCS1 requires the function of both its SH2 and SOCS box domains. For further details about SOCS1 interaction with MA and NC and SOCS1-enhanced particle production, see supporting information (SI) *Text*.

To examine the morphological aspects of HIV-1 particle production, transmission electron microscopy (TEM) was performed. 293T cells that had been cotransfected with pNL4-3, and either a control vector or a SOCS1 expression construct, were subjected to TEM analysis after fixation in glutaraldehyde. In SOCS1-transfected cells, a significantly increased number of mature virus particles was observed on the surfaces of PM compared with the control vector-transfected cells (Fig. 1*E*). There were also no obvious malformations of the virus particles in SOCS1-expressing cells, such as doublet formation or tethering to PM, which are characteristic of particle budding arrest (14) (Fig. 1*E*). Consistent with this observation, virions from SOCS1-transfected cells were found to be infectious as control viruses in Jurkat cells when the same amounts of virus were infected (Fig. 1*F*). These results together indicate that SOCS1 enhances mature and infectious HIV-1 particle formation.

To elucidate the specific step in HIV-1 production that is enhanced by SOCS1, we next performed gene reporter assays using either luciferase expression constructs under the control of wild-type HIV-LTR (pLTR-luc), or a full-length provirus vector (pNL4-3-luc) (15). Interestingly, SOCS1 overexpression was found not to affect the transcription of these reporter constructs (data not shown), indicating that SOCS1 enhances HIV-1 replication via posttranscriptional mechanisms during virus production.

SOCS1 Interacts with the HIV-1 Gag Protein. The results of our initial experiments indicated that SOCS1 enhances HIV-1 production via a posttranscriptional mechanism. We therefore next tested whether SOCS1 could bind directly to HIV-1 Gag. GST pull-down analysis using C-terminal FLAG-tagged p55 Gag (codon-optimized) and GST-fused SOCS1 revealed that p55 Gag undergoes specific coprecipitation with GST-SOCS1 (Fig. 2*A*). Furthermore, both ectopically expressed myc-tagged SOCS1 and endogenous SOCS1 were found to undergo coimmunoprecipitation with Gag-FLAG in 293T cells (Fig. 2 *B* and *C*). Additionally, GST pull-down analysis with various SOCS1 mutants, as depicted in Fig. 2*D*, further demonstrated that a mutant lacking the both N-terminal and SH2 domain (ΔN-SH2) could not bind

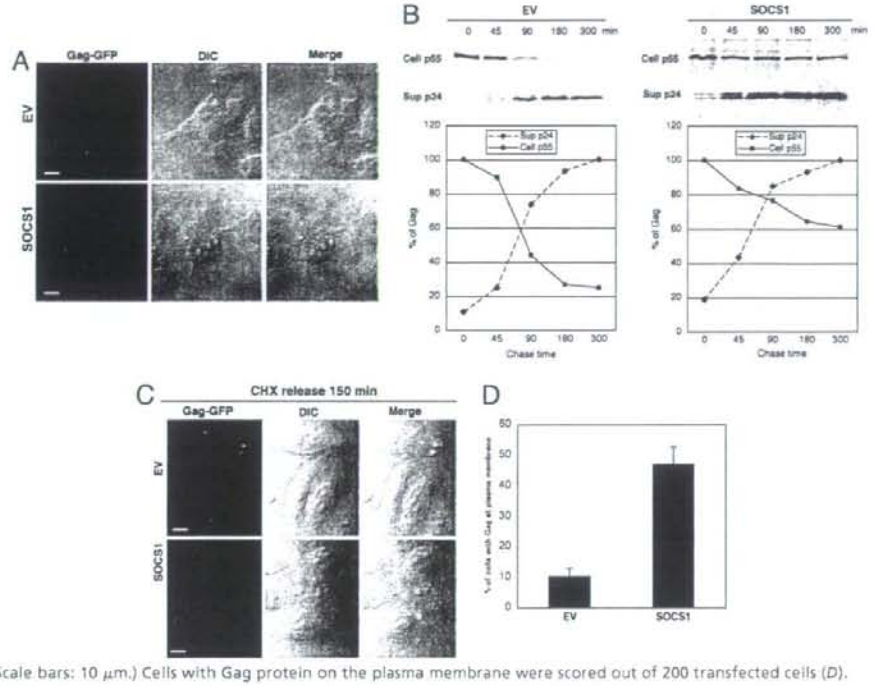

Fig. 3. SOCS1 enhances both the stability and trafficking of HIV-1 Gag. (*A*) HeLa cells cotransfected with pNL4-3 and either control vector (EV) or SOCS1 were immunostained with antibodies targeting anti-p24 (CA). Confocal microscopy with differential interference contrast (DIC) was then performed. (Scale bars: 10 μm.) (*B*) 293T cells were transfected with either a control empty vector (EV) (*Left*) or myc-SOCS1 (*Right*) and cotransfected with pNL4-3. After 48 h, cells were pulse-labeled with [^{35}S]methionine or [^{35}S]cysteine for 15 min and chased for the durations indicated. Cell lysates and pelleted supernatant virions were immunoprecipitated with anti-p24 antibodies followed by autoradiography. (*C* and *D*) HeLa cells seeded on poly-L-lysine-coated cover slides were transfected with either vector control or SOCS1. After 24 h, cells were again transfected with Gag-GFP for 3 h and then treated with 100 μg/ml CHX for 5 h to inhibit protein synthesis. This treatment was followed by incubation with fresh medium; then 150 min after the CHX release, cells were fixed and subjected to confocal microscopy (*C*). (Scale bars: 10 μm.) Cells with Gag protein on the plasma membrane were scored out of 200 transfected cells (*D*).

p55 Gag, whereas an N-terminal or a SOCS box deletion did not affect the binding of SOCS1 to Gag in 293T cells (Fig. 2*E*). This finding indicates that the SH2 domain is important for the interaction of SOCS1 with HIV-1 Gag. Interestingly, the R105E mutant of SOCS1, which disrupts the function of the SH2 domain, still binds Gag (Fig. 2*E*), indicating that the Gag–SOCS1 association is independent of the tyrosine phosphorylation of Gag, as is the case for both HPV-E7 and Vav (16, 17).

To elucidate the SOCS1-binding region of the Gag protein, GST pull-downs with various GST-fused Gag domain constructs were performed. SOCS1 was detected in glutathione bead precipitates with GST-wild-type Gag, GST-Δp6, GST-MA, and GST-NC, but not with other domain constructs (Fig. 2*F*), indicating that SOCS1 interacts with Gag via its MA and NC domains. Consistent with these results, the deletion of both the MA and NC domains of p55 Gag (ΔMAΔNC) completely abolishes its interaction with SOCS1 in coimmunoprecipitation experiments (Fig. 2*G*). Furthermore, *in vitro* analysis with purified proteins also demonstrated that SOCS1 can indeed interact with both the MA and NC regions of HIV-1 Gag in the absence of nucleic acids or other proteins (SI Fig. 5).

We next wished to determine the functional interaction domain in HIV-1 Gag through which SOCS1 functions in terms of virus-like particle production. To this end, we used a MA-deleted Gag mutant with an N-terminal myristoyl tag derived from src (ΔMA-src) (18) and also an NC-deleted Gag mutant with a GCN4 leucine zipper in place of NC, which we herein denote as ΔNC-LZ but which has been described as Z_{IL}-p6 (19). Both of these mutants have been shown still to assemble and bud (18, 19). We found that SOCS1 overexpression can still augment the particle formation of both wild-type Gag and ΔNC-LZ but not ΔMA-src (Fig. 2*H*), indicating that the functional interaction between SOCS1 and HIV-1 Gag is in fact mediated through MA.

To confirm further the direct interaction between SOCS1 and Gag in cells, we examined the intracellular localization of these two proteins. Confocal microscopy revealed that endogenous SOCS1 forms dotted filamentous structures in the cytoplasm and that Gag localizes in a very punctate pattern with SOCS1 from the perinuclear regions to the cell periphery (Fig. 2*I*). These data indicate that SOCS1 interacts with HIV-1 Gag in the cytoplasm during HIV-1 particle production.

SOCS1 Promotes both the Stability of Gag and Its Targeting to the Plasma Membrane. Because we had found from our initial data that SOCS1 increases HIV-1 particle production as a result of its direct interaction with intracellular Gag proteins, we next addressed whether SOCS1 positively regulates Gag stability and subsequent trafficking to PM. Our immunofluorescent analysis with the anti-p24 (CA) antibody initially revealed that SOCS1 overexpression increases the levels of Gag at PM when cotransfected with pNL4-3 at 48 h after transfection, although it was detected at PM in both control and SOCS1-expressing cells (Fig. 3*A*). Furthermore, the levels of cytoplasmic Gag were found to be much lower in the SOCS1-expressing cells compared with the control cells (Fig. 3*A*). These results indicate that SOCS1 enhances Gag trafficking to PM.

To examine next whether SOCS1 affects the stability and trafficking of newly synthesized Gag proteins, we performed pulse–chase analysis. This experiment revealed that SOCS1 significantly increases the stability of the intracellular p55 Gag polyprotein as well as the levels of p24 in the supernatant (Fig. 3*B*). Importantly, p24 was detectable at an earlier time point and reached maximum levels in a shorter period in the cell supernatant of SOCS1-transfected cells compared with control vector-transfected cells (Fig. 3*B*). This finding again suggests that SOCS1 facilitates the intracellular trafficking of newly synthesized Gag proteins to PM.

To confirm this hypothesis further, we performed cycloheximide (CHX) analysis with HeLa cells transfected using either vector control or SOCS1. After 24 h, cells were again transfected with Gag-GFP for 3 h and treated with CHX for 5 h to inhibit protein synthesis. Cells were then cultured in fresh medium without CHX for an additional 150 min and subjected to confocal microscopy. At

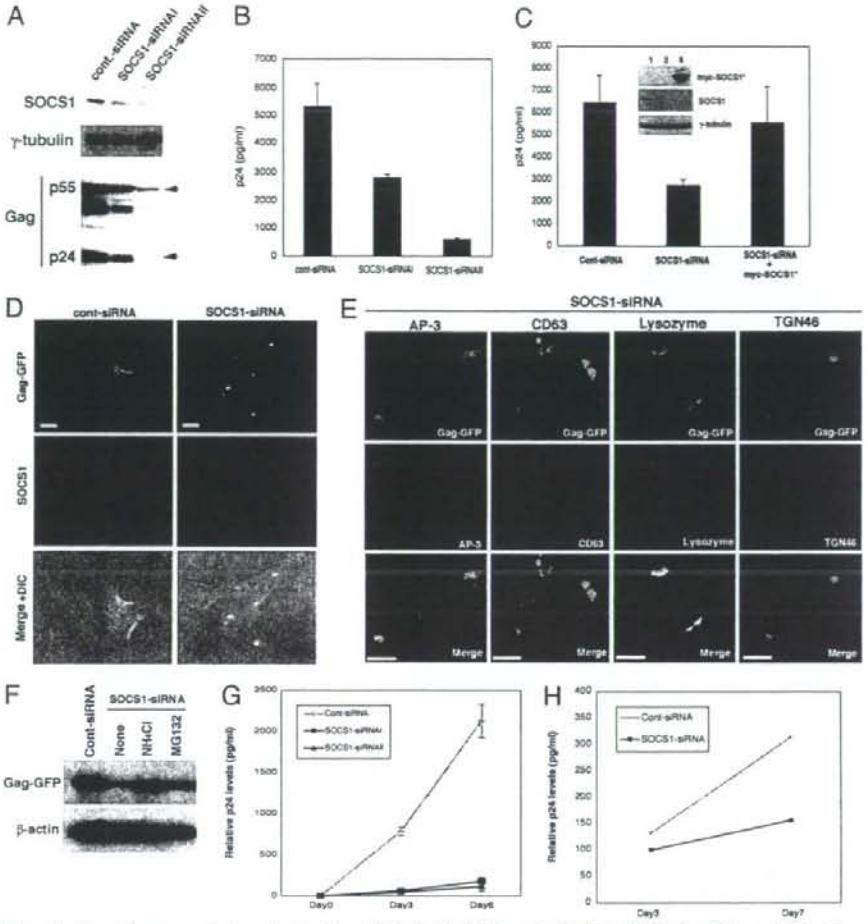

Fig. 4. The targeted inhibition of SOCS1 suppresses Gag trafficking and HIV-1 particle production and enhances Gag degradation in lysosomes. (*A* and *B*) 293T cells were transfected with either control siRNA or two different SOCS1-specific siRNAs (I or II) together with pNL4-3. At 48 h after transfection, cell lysates were subjected to immunoblotting analysis with the indicated antibodies (*A*). Cell supernatants were then subjected to ELISA analysis of p24 levels (*B*). (*C*) 293T cells were transfected with pNL4-3 and cotransfected with control-siRNA, SOCS1-siRNAI alone, or SOCS1-siRNAI plus siRNA-resistant myc-SOCS1 (myc-SOCS1*). After 48 h, cell supernatants were collected and subjected to p24 ELISA. (*Inset*) Immunoblots of the cell lysates. (*D*) HeLa cells were transfected with control or SOCS1-specific siRNA and cotransfected with GFP-Gag. At 48 h after transfection, the cells were subjected to confocal microscopy. (*E*) HeLa cells were transfected with Gag-GFP and SOCS1-siRNA constructs for 48 h. Cells were then fixed and subjected to immunofluorescent analysis with indicated antibodies followed by DAPI staining. (Scale bars: 10 mm.) (*F*) HeLa cells were transfected with Gag-GFP and cotransfected with either control-siRNA or SOCS1-siRNA. After 36 h, the cells were treated with a mock solution, 10 mM NH_4Cl or 10 μM MG132 for another 16 h. Cell were then harvested and subjected to immunoblotting analysis with anti-GFP or anti-β-actin antibodies. (*G*) Jurkat cells were infected with a retroviral vector encoding control (Cont) or two different SOCS1-specific siRNAs (I or II). After selection with puromycin, the cells were then infected with HIV-1_{NL4-3} (multiplicity of infection, 0.1), and p24 antigen levels in cell supernatant were measured by ELISA at the indicated time points. (*H*) Human primary CD4 T cells were separated from healthy donors and infected with lentivirus vectors encoding either control- or SOCS1-siRNAI. The cells were then infected with HIV-1_{NL4-3} (multiplicity of infection, 0.1), and p24 antigen levels in cell supernatant were measured by ELISA at the indicated time points.

this time point, Gag-GFP was found to localize predominantly in a perinuclear region in the control cells (Fig. 3*C*), whereas almost half of the SOCS1-transfected cells exhibited Gag-GFP localization on PM (Fig. 3*D*). These results again indicate that SOCS1 efficiently enhances the trafficking of newly synthesized Gag protein to PM.

The Targeted Disruption of SOCS1 Inhibits Gag Trafficking and HIV-1 Particle Production. To delineate further the role of SOCS1 in the trafficking of Gag and in subsequent HIV-1 particle production, we depleted cellular SOCS1 by siRNA. The significant depletion of SOCS1 expression by two different SOCS1-specific siRNA constructs was confirmed by immunoblotting analysis (Fig. 4 *A* and *B*). Significantly, in cells cotransfected with pNL4-3 and SOCS1-specific siRNAs, both HIV-1 particle release and the levels of intracellular Gag protein are significantly decreased compared with the control cells (Fig. 4 *A* and *B*). Furthermore, the effects of SOCS1-siRNA on the inhibition of HIV-1 particle production was diminished by reexpression with a codon-optimized SOCS1 construct that is resistant to these siRNAs (Fig. 4*C*), indicating that the SOCS1 siRNA suppression of HIV-1 particle production depends on the availability of endogenous SOCS1.

Consistent with these observations, immunofluorescent analysis further revealed that the expression of SOCS1-siRNA dramatically inhibits Gag trafficking such that Gag proteins accumulate in the perinuclear regions as large solid aggregates, as has been reported (20) (Fig. 4*D*). This finding indicates that SOCS1 plays an essential role in the Gag trafficking from perinuclear clusters to PM. Interestingly, these discrete perinuclear clusters of Gag were found to colocalize with lysosome markers, lysozyme, and partly with AP-3, but neither with the late endosome MVB marker CD63 nor the *trans*-Golgi marker TGN46, indicating that Gag is targeted for degradation by lysosomes when the function of SOCS1 is inhibited (Fig. 4*E*). In support of this notion, the levels of intracellular Gag were found to be significantly increased by treatment with a lysosome inhibitor NH_4Cl but not by a proteasome inhibitor MG132 in SOCS1-siRNA cells (Fig. 4*F*), further indicating that the perinuclear clusters of Gag will undergo lysosomal degradation rather than proteasomal degradation when optimal Gag transport to PM is suppressed by the inhibition of SOCS1.

We next addressed whether targeted SOCS1 inhibition would affect HIV-1 particle production in human T cells. The effect of SOCS1 depletion was clearly evident in both HIV-1_{NL4-3}-infected

Jurkat cells and human primary CD4+ T cells, which demonstrated pronounced decreases in virus particle production in SOCS1-siRNA-expressed cells compared with the controls (Fig. 4 *G* and *H*). These results together indicate that the specific inhibition of SOCS1 suppresses the optimal trafficking of Gag to PM, resulting in the degradation of Gag in lysosomes, which in turn leads to the efficient and reproducible inhibition of HIV-1 particle production in various types of human cells.

Discussion

In this work, we report that SOCS1 is an inducible host factor during HIV-1 infection and plays a key role in the late stages of the viral replication pathway via an IFN-independent mechanism (SI Fig. 6). These results represent evidence that SOCS1 is a potent host factor that facilitates HIV-1 particle production via posttranscriptional mechanisms.

SOCS1 has been shown to be a suppressor of several cytokine signaling pathways, and like all SOCS family members it has a central SH2 domain and a conserved C-terminal domain known as the SOCS box (21, 22). Structure–function analyses have further demonstrated that the SOCS1 SH2 domain is required for the efficient binding of its substrates (23, 24). Indeed, our current analyses have also revealed that the SH2 domain of SOCS1 is required for its interaction with the HIV-1 Gag protein. We have shown from our present data that the SOCS box is also required for SOCS1 to function during HIV-1 particle production.

The SOCS box-mediated function of SOCS1 is chiefly exerted via its ubiquitin ligase activity (21, 25). Biochemical binding studies have shown that the SOCS box of SOCS1 interacts with the elongin BC complex, a component of the ubiquitin/proteasome pathway that forms an E3 ligase with Cul2 (or Cul5) and Rbx-1 (21, 26, 27). We show from our current experiments that the SOCS box is required for HIV-1 particle production, indicating the involvement of the ubiquitin/proteasome pathway. However, it is still unknown whether SOCS1 promotes the ubiquitination of Gag and, if so, whether the mono- or poly-ubiquitination of Gag would affect its trafficking and protein stability. Further studies will be necessary to clarify the biological significance of Gag ubiquitination.

Perlman and Resh (20) recently reported that newly synthesized Gag first appears to be diffusely distributed in the cytoplasm, accumulates in perinuclear clusters, passes transiently through a MVB-like compartment, and then traffics to PM. Consistent with these observations, our current work also shows that Gag is accumulated at perinuclear clusters as solid aggregates when its targeting to PM is impaired because of the SOCS1 inhibition.

Another aspect of SOCS1 function during HIV-1 infection was proposed recently. Song *et al.* (28) reported that SOCS1-silenced dendritic cells broadly induce the enhancement of HIV-1 Env-specific CD8+ cytotoxic T lymphocytes and CD4+ T helper cells as well as an antibody response. The induction of the SOCS1 gene in HIV-1 infected cells might therefore disrupt a specific intracellular immune response to HIV-1 in infected host cells.

Based on the strong evidence that we present in our current work that SOCS1 positively regulates the late stages of HIV replication, we conclude that SOCS1 is likely to be a valuable therapeutic target not only for future treatments of AIDS and related diseases, but also for a postexposure prophylaxis against disease in HIV-1-infected individuals.

Materials and Methods

Antibodies and Fluorescent Reagents. Antibodies and fluorescent reagents were obtained from the following sources. Anti-CD63, anti-AP-3, anti-myc (A-14), and anti-SOCS1 (H-93) were from Santa Cruz Biotechnology. Anti-SOCS1 was from Zymed Laboratories. Anti-FLAG (M2) and anti-HA (12CA5) were from Sigma and Roche Diagnostics, respectively. Anti-HIV-p24 (Dako; Cytomation), anti-STAT1, and anti-phospho-STAT1 (Y701) were from BD Transduction Laboratories. Sheep polyclonal anti-TGN46 was from GeneTex.

Plasmid Constructs. Expression constructs for SOCS1 have been described in ref. 29. GST fusion constructs with specific regions derived from the codon-optimized *gag* were generated (MA, CA, NC, p6, Δp6, full-length Gag) by cloning into pGEX-2T (GE Healthcare Bio-Sciences) as described in ref. 30. For retrovirus-mediated siRNA expression, pSUPER.retro.puro vector was digested, as described in ref. 31, with the following sequences: SOCS1-siRNAI, TCGAGCTGCTGGAGCACTA; SOCS1-siRNAII, GGCCAGAACCTTCCTCCTCTT; control siRNA, TCGTATGTTGTGTGGAATT.

Electron Microscopy. Transfected 293T cells were fixed with 2.5% glutaraldehyde and subjected to TEM, as described (14, 32).

ACKNOWLEDGMENTS. We thank Dr. H Gottlinger (University of Massachusetts) for providing plasmids. This work was supported in part by grants from the Ministry of Education, Culture, Sports, Science, and Technology of Japan and Human Health Science of Japan.

1. Sorin M, Kalpana GV (2006) *Curr HIV Res* 4:117–130.
2. Freed EO (2004) *Trends Microbiol* 12:170–177.
3. Peterlin BM, Trono D (2003) *Nat Rev Immunol* 3:97–107.
4. Trkola A (2004) *Curr Opin Microbiol* 7:555–559.
5. Freed EO (1998) *Virology* 251:1–15.
6. Adamson CS, Jones IM (2004) *Rev Med Virol* 14:107–121.
7. VerPlank L, Bouamr F, LaGrassa TJ, Agresta B, Kikonyogo A, Leis J, Carter CA (2001) *Proc Natl Acad Sci USA* 98:7724–7729.
8. Garrus JE, von Schwedler UK, Pornillos OW, Morham SG, Zavitz KH, Wang HE, Wettstein DA, Stray KM, Cote M, Rich RL, *et al.* (2001) *Cell* 107:55–65.
9. Strack B, Calistri A, Craig S, Popova E, Gottlinger HG (2003) *Cell* 114:689–699.
10. Dong X, Li H, Derdowski A, Ding L, Burnett A, Chen X, Peters TR, Dermody TS, Woodruff E, Wang JJ, *et al.* (2005) *Cell* 120:663–674.
11. Alroy I, Tuvia S, Greener T, Gordon D, Barr HM, Taglicht D, Mandil-Levin R, Ben-Avraham D, Konforty D, Nir A, *et al.* (2005) *Proc Natl Acad Sci USA* 102:1478–1483.
12. Ryo A, Suzuki Y, Ichiyama K, Wakatsuki T, Kondoh N, Hada A, Yamamoto M, Yamamoto N (1999) *FEBS Lett* 462:182–186.
13. Adachi A, Gendelman HE, Koenig S, Folks T, Willey R, Rabson A, Martin MA (1986) *J Virol* 59:284–291.
14. Demirov DG, Ono A, Orenstein JM, Freed EO (2002) *Proc Natl Acad Sci USA* 99:955–960.
15. Chang TL, Mosoian A, Pine R, Klotman ME, Moore JP (2002) *J Virol* 76:569–581.
16. De Sepulveda P, Okkenhaug K, Rose JL, Hawley RG, Dubreuil P, Rottapel R (1999) *EMBO J* 18:904–915.
17. Kamio M, Yoshida T, Ogata H, Douchi T, Nagata Y, Inoue M, Hasegawa M, Yonemitsu Y, Yoshimura A (2004) *Oncogene* 23:3107–3115.
18. Gallina A, Mantoan G, Rindi G, Milanesi G (1994) *Biochem Biophys Res Commun* 204:1031–1038.
19. Accola MA, Strack B, Gottlinger HG (2000) *J Virol* 74:5395–5402.
20. Perlman M, Resh MD (2006) *Traffic* 7:731–745.
21. Alexander WS (2002) *Nat Rev Immunol* 2:410–416.
22. Marine JC, Topham DJ, McKay C, Wang D, Parganas E, Stravopodis D, Yoshimura A, Ihle JN (1999) *Cell* 98:609–616.
23. Narazaki M, Fujimoto M, Matsumoto T, Morita Y, Saito H, Kajita T, Yoshizaki K, Naka T, Kishimoto T (1998) *Proc Natl Acad Sci USA* 95:13130–13134.
24. Yasukawa H, Misawa H, Sakamoto H, Masuhara M, Sasaki A, Wakioka T, Ohtsuka S, Imaizumi T, Matsuda T, Ihle JN, *et al.* (1999) *EMBO J* 18:1309–1320.
25. Tyers M, Rottapel R (1999) *Proc Natl Acad Sci USA* 96:12230–12232.
26. Kamizono S, Hanada T, Yasukawa H, Minoguchi S, Kato R, Minoguchi M, Hattori K, Hatakeyama S, Yada M, Morita S, *et al.* (2001) *J Biol Chem* 276:12530–12538.
27. Kamura T, Burian D, Yan Q, Schmidt SL, Lane WS, Querido E, Branton PE, Shilatifard A, Conaway RC, Conaway JW (2001) *J Biol Chem* 276:29748–29753.
28. Song XT, Evel-Kabler K, Rollins L, Aldrich M, Gao F, Huang XF, Chen SY (2006) *PLoS Med* 3:e11.
29. Ryo A, Suizu F, Yoshida Y, Perrem K, Liou YC, Wulf G, Rottapel R, Yamaoka S, Lu KP (2003) *Mol Cell* 12:1413–1426.
30. Morikawa Y, Kishi T, Zhang WH, Nermut MV, Hockley DJ, Jones IM (1995) *J Virol* 69:4519–4523.
31. Ryo A, Uemura H, Ishiguro H, Saitoh T, Yamaguchi A, Perrem K, Kubota Y, Lu KP, Aoki I (2005) *Clin Cancer Res* 11:7523–7531.
32. Nagashima Y, Nishihira H, Miyagi Y, Tanaka Y, Sasaki Y, Nishi T, Imaizumi K, Aoki I, Misugi K (1996) *Cancer* 77:799–804.

Traffic 2008; 9: 540–558
Blackwell Munksgaard

doi: 10.1111/j.1600-0854.2007.00700.x

A CD63 Mutant Inhibits T-cell Tropic Human Immunodeficiency Virus Type 1 Entry by Disrupting CXCR4 Trafficking to the Plasma Membrane

Takeshi Yoshida[1], Yuji Kawano[2], Kei Sato[1], Yoshinori Ando[1], Jun Aoki[1], Yoshiharu Miura[1], Jun Komano[3], Yuetsu Tanaka[4] and Yoshio Koyanagi[1,*]

[1]*Laboratory of Viral Pathogenesis, Institute for Virus Research, Kyoto University, Sakyo-ku, Kyoto 606-8507, Japan*
[2]*Department of Neurology, Neurological Institute, Graduate School of Medical Science, Kyushu University, Higashi-ku, Fukuoka 812-8582, Japan*
[3]*AIDS Research Center, National Institute of Infectious Diseases, Shinjuku-ku, Tokyo 162-8640, Japan*
[4]*Department of Immunology, Graduate School of Medicine, University of the Ryukyus, Nishihara, Okinawa 903-0215, Japan*
**Corresponding author: Yoshio Koyanagi, ykoyanag@virus.kyoto-u.ac.jp*

We have discovered that an N-terminal deletion mutant of a membrane protein, CD63, (CD63ΔN) blocks entry of CXCR4-using, T-cell tropic human immunodeficiency virus type 1 (X4 HIV-1) by suppressing CXCR4 surface expression. This suppression was observed for CXCR4 but not for CD4, CCR5, CD25, CD71 or other tetraspanin proteins. The suppression of CXCR4 expression on the plasma membrane appeared to be caused by mislocalization of CXCR4 and exclusive transportation of CXCR4 toward intracellular organelles, mainly late endosomes/lysosomes. Our data suggest that CXCR4 trafficking can be modified in terms of its recruitment to the plasma membrane without enhancing the degradation or arresting vesicular transport of CXCR4.

Key words: cell surface expression, CD63, CXCR4, HIV-1, ligand-independent trafficking

Received 30 November 2007, revised and accepted for publication 27 December 2007, uncorrected manuscript published online 30 December 2007, published online 13 February 2008

It has been formerly shown that some cellular factors have the ability to suppress retroviral replication. Restriction factors, such as APOBEC3G and Trim5α, play a significant role in controlling human immunodeficiency virus type 1 (HIV-1) infection (1), and it is predicted that other cellular factors will also influence HIV-1 replication. Innovative approaches should, therefore, bring to light, as-yet untested, antiviral factors. We have previously reported a cDNA-library-expressing lentiviral vector system used to isolate an inhibitor of HIV-1-induced cytopathic effect (CPE) (2).

HIV-1 infects T cells and macrophages that express surface CD4 and chemokine receptors. CXCR4 is a G-protein-coupled chemokine receptor that acts as a receptor for stromal-cell-derived factor 1 (SDF-1) and one of the co-receptors for HIV-1 (3). SDF-1 has been shown to inhibit X4 HIV-1 infection, probably by promoting removal of CXCR4 from the cell surface via ligand-induced endocytosis (4,5). The endocytosis of CXCR4 from the cell surface occurs through clathrin-coated pits, which results from the binding to β-arrestin and perhaps adaptor protein complex-2 (AP-2) (5–7). The ubiquitination of CXCR4 at the plasma membrane has been shown to facilitate a sorting event leading to its lysosome-dependent degradation (8,9). In general, membrane proteins are synthesized in the endoplasmic reticulum (ER) and the folded proteins are transported through the Golgi apparatus, and undergo modification such as glycosylation. At the *trans*-Golgi network (TGN), mature proteins are subsequently sorted and packaged into specific vesicles destined for the plasma membrane or the endosomes. In the case of lysosome-associated proteins (LAMP), there are two alternative routes from the TGN, one to the plasma membrane and the other to the lysosomes (10). However, it is unclear whether or not CXCR4 can be targeted directly from the TGN to the lysosome. In addition, there has not been a report of any molecule that affects trafficking of CXCR4 to the plasma membrane.

CD63 is a membrane protein belonging to the tetraspanin superfamily, consisting of four transmembrane domains (TM1-4) and two extracellular (EC) domains (1–2). It is widely expressed on the surface of many cell types, forming tetraspanin-enriched microdomains (TEMs) on the plasma membrane with other tetraspanin proteins (11). It is also present in secretory vesicles (12,13) and the membranes of the late endosomes and lysosomes (14,15). At the plasma membrane, CD63 is known to interact with molecules such as integrins (16), a tissue inhibitor of metalloproteinase-1 (17) and syntenin-1 (18), and is thought to regulate signal transduction pathways required for cell adhesion, motility and survival. It was also reported that CD63 is involved with endocytosis of its interaction partners such as the β-subunit of H, K-ATPase (HKβ) (19) or membrane-type 1 matrix metalloproteinase (MT1-MMP) (20). However, its physiological role is still not well understood (21–23).

In this study, by using our screening strategy (2), we identified an N-terminal deletion mutant of CD63 that

belongs to a novel class of HIV-1 entry blockers. This CD63 mutant appeared to suppress CXCR4 on the cell surface by changing CXCR4 intracellular trafficking probably after its dispatch from the TGN. In addition, we found that wild-type CD63 also functions to suppress CXCR4 cell surface expression, which may be a physiological function of the protein.

Results

Isolation of gene encoding an anti-HIV-1 protein

Using a bicistronic lentiviral vector, encoding cDNA and a humanized recombinant green fluorescent protein (hrGFP), we generated a human peripheral blood leukocyte (PBL) cDNA library-transduced $CD4^+$ $CXCR4^+$ T-cell line (MT-4) (2). Although most cells were killed after X4 HIV-1 ($HIV\text{-}1_{NL4\text{-}3}$) infection, some $hrGFP^+$ ($cDNA^+$) cells were found to proliferate continuously for more than 30 days post-infection (dpi), from which it was inferred that these cells were transduced with an anti-HIV-1 cDNA. From these cells, we independently isolated two cDNA clones, each containing a 3′ fragment of *cd63* cDNA spanning nucleotide positions 193 or 228 to the 3′ poly-A sequence (Figure S1). These cDNAs (designated clone 12.03 and clone 12.22, respectively) encode a C-terminal fragment of CD63 that contains 156 amino acid residues (amino acid positions 83–238) initiating from the third methionine (Figure S1). We then confirmed that both clone 12.03 cDNA- and clone 12.22 cDNA-transduced MT-4 cells ($hrGFP^+$) were resistant against HIV-induced CPE (data not shown) and found that there is little expression of HIV-1 antigen on these cells after HIV-1 inoculation (Figure 1A). Thus, we isolated cDNAs as a new inhibitor gene of HIV-1-induced CPE.

To reproduce this inhibition via transduction of the *cd63* gene, we next prepared a wild-type *cd63* cDNA (CD63wt)-expressing lentiviral vector, as well as an N-terminal deletion mutant (CD63ΔN)-expressing lentiviral vector (Figure 1B) encoding a C-terminal fragment of CD63 identical to those of the isolated cDNA clones mentioned above (Figure S1). Western blotting analysis using an anti-CD63 monoclonal antibody (mAb), confirmed that CD63ΔN-expressing lentiviral vector and the two originally-isolated cDNA expressed peptides with identical molecular weight (MW) (data not shown). As CD63 has a tyrosine-based lysosomal sorting motif (LSM; amino acid positions 233–238) that binds to AP-2 μ and AP-3 μ subunits (15), we also prepared an LSM-deleted CD63ΔN mutant (designated CD63ΔNL) (Figure 1B). FLAG-tagged wild-type CD63 (FLAGCD63wt), CD63ΔN (FLAGCD63ΔN), or CD63ΔNL (FLAGCD63ΔNL) DNA was transfected into HeLa-derived MAGIC-5 cells ($CXCR4^+$ $CD4^+$ $CCR5^+$), and expression was confirmed by Western blotting using an anti-FLAG mAb. This revealed that these proteins were heavily glycosylated (Figure 1C). Immunofluorescent analysis using these DNA showed that CD63wt and CD63ΔN was predominantly distributed in the perinuclear region and some CD63ΔN were found in intracellular vesicles (Figure 1D). The majority of CD63ΔNL, however, appeared to accumulate at the plasma membrane with some intracellular staining (Figure 1D, third panel).

Inhibition of HIV-1 infection by transduction of cells with CD63 and CD63 mutants

To examine anti-HIV-1 activity of CD63-transduced cells further, we generated ectopic CD63wt- or CD63 mutant-expressing cells using a bicistronic $H2K^k$-expressing lentiviral vector. Transduction of the gene by this lentiviral vector did not substantially affect cell growth (data not shown). We then evaluated anti-HIV activity using an enhanced GFP (EGFP)-expressing X4 HIV-1 (NL-EGFP) (24). Flow cytometric analyses indicated that HIV-1 infection was clearly inhibited in the CD63wt- and CD63 mutant (i.e. CD63ΔN and CD63ΔNL)-transduced cells compared with untransduced or empty vector-transduced cells. In CD63ΔN-transduced cells, in particular, HIV-1 infection was severely inhibited (Figure 1E, fourth panel). However, when we used a pseudotyped HIV-1 (where the HIV-1 envelope protein was replaced with that of amphotropic Moloney murine leukemia virus, MLV), the infectivity reduction was not observed (Figure 1F), suggesting that this inhibition is virus envelope protein dependent.

We confirmed that CD63ΔN was also able to protect transduced cells against wild-type X4 HIV-1 infection. Following X4 $HIV\text{-}1_{NL4\text{-}3}$ infection, enzyme-linked immunosorbent assays (ELISA) revealed that the level of HIV-1 $p24^{gag}$ protein in the culture supernatant of CD63ΔN-transduced MT-4 and MAGIC-5 cells was approximately 100-fold lower than that of either empty vector-transduced or untransduced cells (Figure 1G, left and center panels). However, in the case of CCR5-using HIV-1 (R5 HIV-1; $HIV\text{-}1_{JR\text{-}CSF}$) infection, there was no apparent effect of CD63ΔN on the concentration of $p24^{gag}$ in the culture supernatant (Figure 1G, right panel). These data suggest that replication of X4 HIV-1 was specifically inhibited by CD63ΔN. In addition, the level of newly synthesized X4 HIV-1 cDNA in the CD63ΔN-transduced cells was clearly lower (Figure 1H), suggesting that entry of X4 HIV-1 was inhibited by CD63ΔN. Taken together, these results suggest that ectopic CD63wt and CD63ΔN specifically inhibit X4 HIV-1 entry. Therefore, we hypothesized that expression of the X4 virus-specific co-receptor molecule, CXCR4, might be downregulated by ectopic expression of CD63wt and CD63ΔN.

Suppression of CXCR4 surface expression by CD63- and its mutant transduction

To examine the correlation between levels of CXCR4 surface expression and the transduction efficiency of CD63wt and its mutants, we transduced CD63 into cells in different multiplicity of infection (MOI) using a bicistronic $H2K^k$-expressing lentiviral vector. Flow cytometric analysis using an anti-$H2K^k$ mAb confirmed that higher MOI increased transduction efficiency (data not shown). The flow cytometric analyses using an anti-CXCR4 mAb (A-80)